symmetry

MDPI

Article

Well Posedness and Finite Element Approximability of Three-Dimensional Time-Harmonic Electromagnetic Problems Involving Rotating Axisymmetric Objects

Praveen Kalarickel Ramakrishnan † and Mirco Raffetto *,†

Department of Electrical, Electronic, Telecommunications Engineering and Naval Architecture, University of Genoa, Via Opera Pia 11a, I–16145 Genoa, Italy; pravin.nitc@gmail.com

* Correspondence: mirco.raffetto@unige.it; Tel.: +39-010-3352796

† These authors contributed equally to this work.

Received: 6 December 2019; Accepted: 19 January 2020; Published: 2 February 2020

Abstract: A set of sufficient conditions for the well posedness and the convergence of the finite element approximation of three-dimensional time-harmonic electromagnetic boundary value problems involving non-conducting rotating objects with stationary boundaries or bianisotropic media is provided for the first time to the best of authors' knowledge. It is shown that it is not difficult to check the validity of these conditions and that they hold true for broad classes of practically important problems which involve rotating or bianisotropic materials. All details of the applications of the theory are provided for electromagnetic problems involving rotating axisymmetric objects.

Keywords: electromagnetic scattering; time-harmonic electromagnetic fields; moving media; rotating axisymmetric objects; bianisotropic media; variational formulation; well posedness; finite element method; convergence of the approximation

1. Introduction

The presence of rotating objects in electromagnetic problems is of interest in several applications, ranging from the detection of helicopters to the tachometry of celestial bodies [1,2]. Unfortunately, as an immediate consequence of the presence of materials in motion, all these electromagnetic problems are difficult to solve. This is a consequence of the fact that all moving media are perceived as bianisotropic [3,4].

Independently of the motion, bianisotropic media have been considered in several recent investigations, in particular in the context of metamaterials, with frequencies belonging to the microwave band or to the photonic one [5–8], for their huge potentialities or for their practical applications.

The complexity of electromagnetic problems involving media in motion or bianisotropic materials prevents any chance of getting results without the use of numerical simulators. However, in order to rely on them, it is important to know a priori results of well posedness of the problems of interest and on their numerical approximability. A few papers addressing these topics have been recently published [9–12]. However, due to the difficulty of the problems considered, most of them present results under some restrictive hypotheses. For example, in [9], the results of interest are deduced by exploiting in a crucial way the presence of losses, while in [10] the authors study cylinders in axial motions. In [11], a problem of evolution is studied inside a cavity, preventing the exploitation of the results in many applications and, finally, in [12] the constitutive parameters are smooth so neglecting the possibility of considering radiation or scattering problems.

In this paper, we try to overcome most of these limitations by extending the theory developed in [10] to three-dimensional time-harmonic electromagnetic boundary value problems involving lossy or lossless materials which can be bianisotropic or in motion. Only on the materials in motion will we consider some restrictions. In particular, in order to retain the possibility to perform the analysis of time-harmonic problems, we need that the boundaries of the moving objects are stationary [3]. Thus, we will restrict ourselves to consider the rotation of axisymmetric objects. For the same reason, the velocity field will be considered independent of time. Moreover, the media in motion have to be non-conductive, in order to avoid the difficulties related to the convective currents, which could become surface electric currents [13] and then determine a discontinuity of the tangential part of the magnetic field.

As for the media involved whose bianisotropy is not due to motion, we do not consider any restrictive hypothesis. In particular, the formulation we consider allows the solution of radiation [14], scattering [1,5,15], or guided wave problems [16,17], which are all of interest for applications.

The well posedness and finite element approximability guaranteed by our theory allow us to obtain reliable solutions from numerical simulations for rotating axisymmetric objects. With this, we can solve several problems. However, for the sake of conciseness, we selected just two representative examples. For one of them, we have approximate semi-analytic solutions [1], and the range of validity of the approximation involved in those solutions can be verified using our approach. Our second example is representative of the majority of problems involving rotating objects, for which no result can be found in the open literature. For any problem of this class, the reliable solution obtained under the conditions required by our theory can serve as a benchmark for other numerical techniques.

The paper is organized as follows. In Section 2, the problems of interest are defined. Section 3 reports the main ideas which can be used to show that the problems of interest are well posed. The results of convergence of Galerkin and finite element approximations are presented in Section 4. In Section 5, we briefly present the main features of the finite element simulator exploited to compute the results presented in Section 7. In these first sections, we heavily exploit the results presented in [9,10,18]. We have included these sections in our manuscript in order to ease readers' task and because the results we present are not trivially deduced from [10,18], since they deal with two-dimensional problems. The main novelties of the paper are presented in Sections 6 and 7. In particular, in Section 6, we present some useful suggestions on how our theory can be exploited to solve problems of practical interest and in Section 7 the practical applications of our theory to rotating axisymmetric objects are presented. The conclusions are reported in Section 8 and some technical details are provided in the appendix.

2. Problem Definition

In this section, we define the time-harmonic electromagnetic boundary value problem we will deal with in the rest of the paper. Most of the considerations of this section are taken from Sections 2 and 3 of [9] and are here reported to ease the reader's task and to introduce some specific considerations of interest for problems involving rotating axisymmetric objects.

To avoid restrictions on the applicability of our analysis, the problem will be formulated on a domain Ω satisfying the following hypotheses ($\Gamma = \partial\Omega$ denotes its boundary):

HD1. $\Omega \subset \mathbb{R}^3$ is open, bounded and connected,
HD2. Γ is Lipschitz continuous and stationary.

Moreover, in order to be able to consider electromagnetic problems of practical interest, different inhomogeneous materials will be taken into account. This is the reason why we assume:

HD3. Ω can be decomposed into m subdomains (non-empty, open and connected subsets of Ω having Lipschitz continuous stationary boundaries) denoted Ω_i, $i \in I = \{1, \ldots, m\}$, satisfying $\overline{\Omega} = \overline{\Omega}_1 \cup \ldots \cup \overline{\Omega}_m$ ($\overline{\Omega}$ is the closure of Ω) and $\Omega_i \cap \Omega_j = \emptyset$ for $i \neq j$.

This hypothesis allows us to consider also the presence of rotating axisymmetric objects.

The specific target of the paper is to deal with electromagnetic problems involving very general materials. However, in order to give a sense to a time-harmonic analysis, we have at least to assume that:

HM1. Any material involved is linear and time-invariant and satisfies the following constitutive relations:

$$\begin{cases} \mathbf{D} = (1/c_0)\, P\, \mathbf{E} + L\, \mathbf{B} & \text{in } \Omega, \\ \mathbf{H} = M\, \mathbf{E} + c_0\, Q\, \mathbf{B} & \text{in } \Omega. \end{cases} \tag{1}$$

In the above equation, **E**, **B**, **D**, **H**, and c_0 are, respectively, the electric field, the magnetic induction, the electric displacement, the magnetic field and the velocity of light in vacuum [19]. L, M, P and Q are four 3-by-3 matrix-valued complex functions defined almost everywhere in Ω. The vector fields **E**, **B**, **D** and **H** are complex valued too, as it is usually the case for electromagnetic field problems in which the real fields depend sinusoidally on time [20] (pp. 13–16). Equation (1) implicitly takes account of the electric current densities, as usual. Other equivalent forms of the above constitutive equations are possible [21] (p. 49) [22], and will also be used later on.

Different inhomogeneous bianisotropic materials will be modeled by assuming the following hypothesis.

HM2. The matrix valued complex functions representing the effective constitutive parameters satisfy [23] (p. 3), [24] (p. 36):

$$P|_{\Omega_k}, Q|_{\Omega_k}, L|_{\Omega_k}, M|_{\Omega_k} \in (C^0(\overline{\Omega}_k))^{3\times 3},\ \forall k \in I$$

Such hypothesis is in no way restrictive for all applications of interest since the material properties are just piecewise but not globally continuous. In particular, as we will verify later on, hypotheses HM1 and HM2 do not exclude the presence of rotating axisymmetric objects [2] either.

The following additional notations and hypotheses are necessary too. $(L^2(\Omega))^3$ is the usual Hilbert space of complex-valued square integrable vector fields on Ω and with scalar product given by $(\mathbf{u}, \mathbf{v})_{0,\Omega} = \int_\Omega \mathbf{v}^* \mathbf{u}\, dV$ (* denotes the conjugate transpose). $H(\mathrm{curl}, \Omega) = \{\mathbf{v} \in (L^2(\Omega))^3 \mid \mathrm{curl}\, \mathbf{v} \in (L(\Omega))^3\}$ [24] (p. 55). The space where we will seek **E** and **H** is [24] (p. 82; see also p. 69)

$$U = H_{L^2,\Gamma}(\mathrm{curl}, \Omega) = \{\mathbf{v} \in H(\mathrm{curl}, \Omega) \mid \mathbf{v} \times \mathbf{n} \in L_t^2(\Gamma)\}, \tag{2}$$

where [24] (p. 48)

$$L_t^2(\Gamma) = \{\mathbf{v} \in (L^2(\Gamma))^3 \mid \mathbf{v} \cdot \mathbf{n} = 0 \ \text{ almost everywhere on } \Gamma\}. \tag{3}$$

The scalar products in $L_t^2(\Gamma)$ and U are respectively given by $(\mathbf{u}, \mathbf{v})_{0,\Gamma} = \int_\Gamma \mathbf{v}^* \mathbf{u}\, dS$ and [24] (p. 84, p. 69)

$$(\mathbf{u}, \mathbf{v})_{U,\Omega} = (\mathbf{u}, \mathbf{v})_{0,\Omega} + (\mathrm{curl}\, \mathbf{u}, \mathrm{curl}\, \mathbf{v})_{0,\Omega} + (\mathbf{u} \times \mathbf{n}, \mathbf{v} \times \mathbf{n})_{0,\Gamma}. \tag{4}$$

The induced norm is $\|\mathbf{u}\|_U = (\mathbf{u}, \mathbf{u})_{U,\Omega}^{1/2}$.

The symbol ω represents the angular frequency, as usual. Moreover, $\mathbf{J}_e$ and $\mathbf{J}_m$ are the electric and magnetic current densities, respectively, prescribed by the sources, Y is the scalar admittance involved in impedance boundary condition and $\mathbf{f}_R$ is the corresponding inhomogeneous term. Finally, the admittance function Y with domain Γ and range in $\mathbb{C}$ is assumed to satisfy

HB1. Y is piecewise continuous and $|Y|$ is bounded.

We are now in a position to state the electromagnetic boundary value problem we will address in this paper.

Problem 1. *Under the hypotheses HD1-HD3, HM1-HM2, HB1, given* $\omega > 0$, $\mathbf{J}_e \in (L^2(\Omega))^3$, $\mathbf{J}_m \in (L^2(\Omega))^3$ *and* $\mathbf{f}_R \in L_t^2(\Gamma)$, *find* $(\mathbf{E}, \mathbf{B}, \mathbf{H}, \mathbf{D}) \in U \times (L^2(\Omega))^3 \times U \times (L^2(\Omega))^3$ *satisfying (1) and the following equations:*

$$\begin{cases} \operatorname{curl} \mathbf{H} - j\omega\, \mathbf{D} = \mathbf{J}_e & \text{in } \Omega, \\ \operatorname{curl} \mathbf{E} + j\omega\, \mathbf{B} = -\mathbf{J}_m & \text{in } \Omega, \\ \mathbf{H} \times \mathbf{n} - Y\left(\mathbf{n} \times \mathbf{E} \times \mathbf{n}\right) = \mathbf{f}_R & \text{on } \Gamma. \end{cases} \tag{5}$$

As it was pointed out in [9], such a model can be thought of as an approximation of a radiation or scattering problem, or as a realistic formulation of a cavity problem.

The following variational formulation of Problem 1 was derived in [9]:

Problem 2. *Under the hypotheses HD1–HD3, HM1–HM2, HB1, given* $\omega > 0$, $\mathbf{J}_e \in (L^2(\Omega))^3$, $\mathbf{J}_m \in (L^2(\Omega)^3$ *and* $\mathbf{f}_R \in L_t^2(\Gamma)$, *find* $\mathbf{E} \in U$ *such that*

$$a(\mathbf{E}, \mathbf{v}) = l(\mathbf{v}) \;\; \forall \mathbf{v} \in U, \tag{6}$$

where

$$\begin{aligned} a(\mathbf{u}, \mathbf{v}) = c_0 \left(Q \operatorname{curl} \mathbf{u}, \operatorname{curl} \mathbf{v}\right)_{0,\Omega} - \frac{\omega^2}{c_0} \left(P\, \mathbf{u}, \mathbf{v}\right)_{0,\Omega} - j\omega \left(M\, \mathbf{u}, \operatorname{curl} \mathbf{v}\right)_{0,\Omega} \\ - j\omega \left(L \operatorname{curl} \mathbf{u}, \mathbf{v}\right)_{0,\Omega} + j\omega \left(Y\, (\mathbf{n} \times \mathbf{u} \times \mathbf{n}), \mathbf{n} \times \mathbf{v} \times \mathbf{n}\right)_{0,\Gamma} \end{aligned} \tag{7}$$

and

$$l(\mathbf{v}) = -j\omega \left(\mathbf{J}_e, \mathbf{v}\right)_{0,\Omega} - c_0 \left(Q\, \mathbf{J}_m, \operatorname{curl} \mathbf{v}\right)_{0,\Omega} + j\omega \left(L\, \mathbf{J}_m, \mathbf{v}\right)_{0,\Omega} - j\omega \left(\mathbf{f}_R, \mathbf{n} \times \mathbf{v} \times \mathbf{n}\right)_{0,\Gamma}. \tag{8}$$

It was shown in [9] that the two formulations are equivalent, in the sense that, from the solution of Problem 1, one can deduce the solution of Problem 2 and vice versa; moreover, the well posedness of the former implies the well posedness of the latter and vice versa [9].

3. Well Posedness of the Problem

Following the main ideas presented in Section 4 of [10], in this section, we prove the well posedness of the three-dimensional problems of interest. The target will be achieved by showing that, under appropriate additional hypotheses, we can apply the generalized Lax-Milgram lemma [24] (p. 21) to Problem 2.

The continuity of the sesquilinear and antilinear forms, a and l, are easily deduced under the hypotheses already introduced (HD1-HD3, HM1-HM2, HB1). Thus, it remains to introduce the additional hypotheses allowing us to prove that the sesquilinear form a satisfies the following conditions:

$$\text{for every } \mathbf{v} \in U, \mathbf{v} \neq 0, \quad \sup_{\mathbf{u} \in U} |a(\mathbf{u}, \mathbf{v})| > 0, \tag{9}$$

$$\text{we can find } \alpha : \inf_{\mathbf{u} \in U,\ \|\mathbf{u}\|_U = 1} \sup_{\mathbf{v} \in U,\ \|\mathbf{v}\|_U \leq 1} |a(\mathbf{u}, \mathbf{v})| \geq \alpha > 0. \tag{10}$$

We establish under which hypotheses these conditions hold true in the following subsections.

3.1. Hypotheses to Prove Condition (9)

Condition (9) is easily proved once we know that the solution to Problem 2 is unique, as shown in [10]. In turn, uniqueness for Problem 2 is achieved by proving uniqueness for the corresponding homogeneous problem (that is the one with $l = 0$) [25] (p. 20), [24] (p. 92). Finally, uniqueness for the corresponding homogeneous problem can be deduced by a standard technique [26] (pp. 187–203), [10,24,27] (p. 92), in the presence of some losses and by unique continuation results.

In the following, we introduce the hypotheses which allow for getting the result of interest in this subsection. In order to let the reader understand the general picture, we observe that:

- the first group of hypotheses (HM3 and HB2) requires that the media and the boundary do not provide active power,
- the second group of assumptions (HM4–HM7 and HB3) asks for the presence of some losses in the media or on the boundary or the invertibility of the constitutive matrix P, $\forall \mathbf{x} \in \overline{\Omega}_i, \forall i \in I$,
- the first two groups of hypotheses are sufficient to prove that the solution of the homogeneous problem is zero on a subdomain of Ω or that its tangential part on a subset of the boundary is zero,
- the third group of assumptions (HM8–HM12) guarantee the applicability of a unique continuation result, allowing us to show that condition (9) holds true.

In order to write our assumptions, we need to introduce some additional notation.
In [9], it was shown that the sesquilinear form a can be recast is the form

$$a(\mathbf{u},\mathbf{v}) = \int_\Omega \left\{ (\mathbf{v}^*, \operatorname{curl} \mathbf{v}^*)\, A \begin{pmatrix} \mathbf{u} \\ \operatorname{curl} \mathbf{u} \end{pmatrix} \right\} + j\omega \big(Y\, \mathbf{n} \times \mathbf{u} \times \mathbf{n}, \mathbf{n} \times \mathbf{v} \times \mathbf{n} \big)_{0,\Gamma}, \tag{11}$$

where

$$A = \begin{pmatrix} -\frac{\omega^2}{c_0} P & -j\omega L \\ -j\omega M & c_0 Q \end{pmatrix} = A_s - jA_{ss}, \tag{12}$$

being [9] $A_s = \frac{A+A^*}{2}$ and $A_{ss} = \frac{A^*-A}{2j}$. For future use, the vector notation introduced in Equation (11) is generalized as follows for the ordered pair $\mathbf{q}, \mathbf{r} \in \mathbb{C}^3$:

$$\mathbf{p} = \begin{pmatrix} \mathbf{q} \\ \mathbf{r} \end{pmatrix}. \tag{13}$$

Moreover, by referring to the constitutive relation (1) or the above definition of A, we introduce a splitting of the subscript $i \in I$ of the subdomains Ω_i: $i \in I_a$ when $L = M = 0\ \forall \mathbf{x} \in \Omega_i$ (the media are anisotropic), otherwise $i \in I_b$. Finally, an alternative form of the constitutive relations will be used to state unique continuation results. Such an alternative form is

$$\begin{cases} \mathbf{E} = \kappa\, \mathbf{D} + \chi\, \mathbf{B} & \text{in } \Omega, \\ \mathbf{H} = \gamma\, \mathbf{D} + \nu\, \mathbf{B} & \text{in } \Omega, \end{cases} \tag{14}$$

where the constitutive matrices $\kappa = c_0\, P^{-1}$, $\chi = -c_0\, P^{-1}\, L$, $\gamma = c_0\, M\, P^{-1}$ and $\nu = c_0\, (Q - M\, P^{-1}\, L)$ [22] are all well defined where P^{-1} is well defined (see hypothesis HM7 below).

The first group of hypotheses is the following:

HM3. $\mathbf{p}^* A_{ss} \mathbf{p} \leq 0$, $\forall \mathbf{p} \in \mathbb{C}^6$, $\forall \mathbf{x} \in \Omega_i$, $\forall i \in I$,

HB2. $Re(Y) \geq 0$ on Γ.

The assumptions of the second group (HM4–HM7 on the media and HB3 on the boundary) are all related to the presence of losses (apart from HM7) and read:

HM4. We can find $K_{dl} > 0$ and $D \subset \Omega_i$, $i \in I$, D open, non-empty such that $\mathbf{p}^* A_{ss} \mathbf{p} \leq -K_{dl}(|\mathbf{q}|^2 + |\mathbf{r}|^2)$ in D,

HM5. We can find $K_{el} > 0$ and $D \subset \Omega_i$, $i \in I$, D open, non-empty such that $\mathbf{p}^* A_{ss} \mathbf{p} \leq -K_{el} |\mathbf{q}|^2$ in D,

HM6. We can find $K_{ml} > 0$ and $D \subset \Omega_i$, $i \in I_a$, D open, non-empty such that $\mathbf{p}^* A_{ss} \mathbf{p} \leq -K_{ml} |\mathbf{r}|^2$ in D,

HM7. P is invertible, for all $\mathbf{x} \in \overline{\Omega}_i$, $\forall i \in I$,

HB3. We can find $C_{Ym} > 0$ and a non-empty open part Γ_l of Γ such that $Re(Y) \geq C_{Ym}$ almost everywhere on Γ_l.

Appropriate combinations of these hypotheses are sufficient to prove (see Lemma A1 in the Appendix A) that any solution of the homogeneous variational problem has a tangential part, which is trivial on Γ_l or is trivial in the subdomain D.

Once this result has been obtained, in order to prove that the field is zero everywhere in Ω, one has to apply unique continuation results [26] (pp. 187–203), [10,24,27] (p. 92). To achieve this target in the presence of anisotropic and bianisotropic media, we refer to [22], and introduce the following third set of hypotheses:

HM8. All entries of $\kappa, \chi, \gamma, \nu \in C^{\infty}(\overline{\Omega}_i)$ and are restrictions of analytic functions in Ω_i, $\forall i \in I$,

HM9. $\exists\exists C_{\kappa,d} > 0$, $C_{\nu,d} > 0 : |determinant\,(\kappa)\,| \geq C_{\kappa,d}$, $|determinant\,(\nu)\,| \geq C_{\nu,d}$, $\forall \mathbf{x} \in \overline{\Omega}_i, \forall i \in I$,

HM10. $\mathbf{l}_{1,3}^T\,\kappa^{-1}\,\mathbf{l}_{1,3} \neq 0$, $\mathbf{l}_{1,3}^T\,\nu^{-1}\,\mathbf{l}_{1,3} \neq 0\ \forall \mathbf{l}_{1,3} \in \mathbb{R}^3, \mathbf{l}_{1,3} \neq 0$, $\forall \mathbf{x} \in \overline{\Omega}_i$, $\forall i \in I_a$,

HM11. $\exists\exists C_{\kappa,r} > 0$, $C_{\nu,r} > 0 :$ $|\mathbf{l}_{1,3,n}^T\,\kappa^{-1}\,\mathbf{l}_{1,3,n}| \geq C_{\kappa,r}$, $|\mathbf{l}_{1,3,n}^T\,\nu^{-1}\,\mathbf{l}_{1,3,n}| \geq C_{\nu,r}\ \forall \mathbf{l}_{1,3,n} \in \mathbb{R}^3 : \|\mathbf{l}_{1,3,n}\|_2 = 1$, $\forall \mathbf{x} \in \overline{\Omega}_i$, $\forall i \in I_b$,

HM12. $\exists\exists C_{\kappa,s} > 0, C_{\nu,s} > 0$:

$$\Big(\sum_{i,j=1}^{3} |\kappa_{ij}|\Big) - \min_{i=1,2,3} |\kappa_{ii}| \leq C_{\kappa,s} \quad \forall \mathbf{x} \in \overline{\Omega}_k,\ \forall k \in I_b, \tag{15}$$

$$\Big(\sum_{i,j=1}^{3} |\nu_{ij}|\Big) - \min_{i=1,2,3} |\nu_{ii}| \leq C_{\nu,s} \quad \forall \mathbf{x} \in \overline{\Omega}_k,\ \forall k \in I_b, \tag{16}$$

and κ, χ, γ and ν satisfy

$$\frac{4\left(\left(\sum_{i,j=1}^{3} |\gamma_{ij}|\right) - \min_{i=1,2,3} |\gamma_{ii}|\right)\left(\left(\sum_{i,j=1}^{3} |\chi_{ij}|\right) - \min_{i=1,2,3} |\chi_{ii}|\right)}{\left(-C_{\kappa,s} + \sqrt{C_{\kappa,s}^2 + 4\,C_{\kappa,d}\,C_{\kappa,r}}\right)\left(-C_{\nu,s} + \sqrt{C_{\nu,s}^2 + 4\,C_{\nu,d}\,C_{\nu,r}}\right)} < 1 \tag{17}$$

$\forall \mathbf{x} \in \overline{\Omega}_k$, $\forall k \in I_b$.

Remark 1. *The constants and the constraints involved in hypotheses HM9, HM11 and HM12 could be defined in any single subdomain Ω_i, $i \in I_b$, in order to deduce less restrictive conditions under which our theory holds true. This approach was exploited for example in [10]. Here, we use constants and constraints defined globally, in order to avoid longer and technically more complicated definitions.*

In particular, with hypotheses HM7, HM8, HM9 and HM10, by Theorem 6.4 of [22], we can conclude that any solution of the homogeneous variational problem is analytic in all anisotropic media, i.e., for all Ω_i, $i \in I_a$. Moreover, under hypotheses HM7, HM8, HM9, HM11 and HM12, by Theorem 7.3 of [22], we get the same result for all Ω_i, $i \in I_b$.

These preliminary outcomes allow us to state the following uniqueness result, which will be proved in Appendix A:

Theorem 1. *Under the hypotheses HD1–HD3, HM1–HM3, HM7–HM9, HB1–HB2, if HM10 is satisfied by the anisotropic media and HM11 and HM12 are satisfied by the bianisotropic materials involved, then Problem 2 admits a unique solution provided that at least one of HM4 or HM5 or HM6 or HB3 is satisfied.*

Like in [10,28], it is now extremely simple to deduce (in Appendix A, it is possible to find the proof; * denotes the complex conjugate)

Theorem 2. *Under the hypotheses HD1–HD3, HM1–HM3, HM7–HM9, HB1–HB2, if HM10 is satisfied by the anisotropic media and HM11 and HM12 are satisfied by the bianisotropic materials involved, then the homogeneous variational problem, find* $\mathbf{v} \in U$ *such that* $(a(\mathbf{u},\mathbf{v}))^* = 0\ \forall \mathbf{u} \in U$*, admits a unique solution* $\mathbf{v} = 0$ *provided that at least one of HM4 or HM5 or HM6 or HB3 is satisfied.*

With this result, we can finally show that, under appropriate hypotheses, condition (9) holds true.

Theorem 3. *Under the hypotheses HD1–HD3, HM1–HM3, HM7–HM9, HB1–HB2, if HM10 is satisfied by the anisotropic media and HM11 and HM12 are satisfied by the bianisotropic materials involved, then condition (9) holds true provided that at least one of HM4 or HM5 or HM6 or HB3 is satisfied.*

Proof. Suppose that (9) is not satisfied. Then, we can find $\mathbf{v} \in U$, $\mathbf{v} \neq 0$ such that $\sup_{\mathbf{u}\in U} |a(\mathbf{u},\mathbf{v})| = 0$. However, $|a(\mathbf{u},\mathbf{v})| = |\,(a(\mathbf{u},\mathbf{v}))^*\,|$. Then, for the indicated $\mathbf{v} \neq 0$, $|\,(a(\mathbf{u},\mathbf{v}))^*\,| = 0\ \forall \mathbf{u} \in U$. This is at odds with Theorem 2, since we have assumed the same hypotheses. □

3.2. Additional Hypotheses to Prove Condition (10)

Under hypothesis HM2 or HB1, by a direct application of the Cauchy–Schwarz inequality, we deduce that it is possible to define the following continuity constants:

- $\exists C_{PL} > 0$: $|(P\,\mathbf{u},\mathbf{v})_{0,\Omega}| \leq C_{PL}\|\mathbf{u}\|_{0,\Omega}\|\mathbf{v}\|_{0,\Omega}$ for all $\mathbf{u},\mathbf{v} \in (L^2(\Omega))^3$,
- $\exists C_L > 0$: $|(L\,\mathrm{curl}\,\mathbf{u},\mathbf{v})_{0,\Omega}| \leq C_L\|\mathrm{curl}\,\mathbf{u}\|_{0,\Omega}\|\mathbf{v}\|_{0,\Omega}$ for all $\mathbf{u} \in H(\mathrm{curl},\Omega)$ and $\mathbf{v} \in (L^2(\Omega))^3$,
- $\exists C_M > 0$: $|(M\,\mathbf{u},\mathrm{curl}\,\mathbf{v})_{0,\Omega}| \leq C_M\|\mathbf{u}\|_{0,\Omega}\|\mathrm{curl}\,\mathbf{v}\|_{0,\Omega}$ for all $\mathbf{u} \in (L^2(\Omega))^3$ and $\mathbf{v} \in H(\mathrm{curl},\Omega)$,
- $\exists C_{YL} > 0$: $|(Y(\mathbf{n}\times\mathbf{u}\times\mathbf{n}),\mathbf{n}\times\mathbf{v}\times\mathbf{n})_{0,\Gamma}| \leq C_{YL}\|\mathbf{n}\times\mathbf{u}\times\mathbf{n}\|_{0,\Gamma}\|\mathbf{n}\times\mathbf{v}\times\mathbf{n}\|_{0,\Gamma}$.

In order to prove condition (10), we introduce the following additional hypotheses, which guarantee that it is possible to find some coercivity constants:

HM13. We can find $C_{PS} > 0$ such that $|(P\mathbf{u},\mathbf{u})_{0,\Omega}| \geq C_{PS}\|\mathbf{u}\|^2_{0,\Omega}$ for all $\mathbf{u} \in (L^2(\Omega))^3$.

HM14. We can find $C_{QS} > 0$ such that $|(Q\mathrm{curl}\,\mathbf{u},\mathrm{curl}\,\mathbf{u})_{0,\Omega}| \geq C_{QS}\|\mathrm{curl}\,\mathbf{u}\|^2_{0,\Omega}$ for all $\mathbf{u} \in H(\mathrm{curl},\Omega)$.

HB3S. We can find $C_{Ym} > 0$ such that $Re(Y) \geq C_{Ym}$ almost everywhere on Γ.

Moreover, we assume:

HM15. C_{PS}, C_{QS}, C_L and C_M (i.e., all media involved) are such that $C_{QS} - \frac{C_L C_M}{C_{PS}} > 0$.

As is shown in Appendix A, it is now possible to get the following result:

Theorem 4. *Under the hypotheses HD1–HD3, HM1–HM3, HM7–HM9, HB1, HB3S, HM13–HM15, if HM10 is satisfied by the anisotropic media and HM11 and HM12 are satisfied by the bianisotropic materials involved, then the sesquilinear form a satisfies condition (10).*

The following theorem, which is the main result of this section, is now a simple consequence:

Theorem 5. *Under the hypotheses HD1–HD3, HM1–HM3, HM7–HM9, HB1, HB3S, HM13–HM15, if HM10 is satisfied by the anisotropic media and HM11 and HM12 are satisfied by the bianisotropic materials involved, then Problem 2 is well posed.*

Proof. HB3S implies HB2 and HB3. It also implies that the logical or of HM4, HM5, HM6 and HB3, which is present as a condition in Theorem 3, is true. Thus, the hypotheses reported in the statement of the theorem guarantee the applicability of Theorems 3 and 4. □

4. Convergence of Galerkin and Finite Element Approximations

Once the result of well posedness of the problems of interest is established, we can proceed as in Sections 5 and 6 of [10], to deduce the conditions under which the convergence of Galerkin [29] and finite element [24] approximations can be guaranteed.

Convergence of an approximation [29] (p. 112) refers to the property of sequences of solutions of the approximate problem and requires that they converge to the unique solution of the problem of interest.

Any sequence of approximate solutions is built by considering a sequence $\{U_h\}$ of finite dimensional subspaces U_h of U. h is a denumerable and bounded set of strictly positive indexes having zero as the only limit point [29] (p. 112).

For any $h \in I$, a set of approximate sources is considered: $\mathbf{J}_{eh}, \mathbf{J}_{mh} \in (L^2(\Omega))^3$ and $\mathbf{f}_{Rh} \in L_t^2(\Gamma)$. With these, we define the following approximate antilinear form:

$$l_h(\mathbf{v}) = -j\omega(\mathbf{J}_{eh}, \mathbf{v})_{0,\Omega} - c_0(Q\,\mathbf{J}_{mh}, \mathrm{curl}\mathbf{v})_{0,\Omega} + j\omega(L\,\mathbf{J}_{mh}, \mathbf{v})_{0,\Omega} - j\omega(\mathbf{f}_{Rh}, \mathbf{n} \times \mathbf{v} \times \mathbf{n})_{0,\Gamma} \tag{18}$$

and the following discrete version of Problem 2.

Problem 3. *Under the hypotheses HD1–HD3, HM1–HM2, HB1, given* $\omega > 0$, $\mathbf{J}_{eh} \in (L^2(\Omega))^3$, $\mathbf{J}_{mh} \in (L^2(\Omega)^3$ *and* $\mathbf{f}_{Rh} \in L_t^2(\Gamma)$, *find* $\mathbf{E}_h \in U_h$ *such that*

$$a(\mathbf{E}_h, \mathbf{v}_h) = l_h(\mathbf{v}_h) \;\; \forall \mathbf{v}_h \in U_h. \tag{19}$$

In order to state the results of interest, it is necessary to introduce the following subspaces of U_h:

$$U_{0h} = \{\mathbf{u}_h \in U_h \,|\, \mathrm{curl}\,\mathbf{u}_h = 0 \text{ in } \Omega \text{ and } \mathbf{u}_h \times \mathbf{n} = 0 \text{ on } \Gamma\}, \tag{20}$$

$$U_{1h} = \{\mathbf{u}_h \in U_h \,|\, (P\mathbf{u}_h, \mathbf{v}_h)_{0,\Omega} = 0 \; \forall \mathbf{v}_h \in U_{0h}\}. \tag{21}$$

On the sequence of approximating space [24,30], we need to consider

HSAS1. $\lim_{h\to 0} \inf_{\mathbf{u}_h \in U_h} \|\mathbf{u} - \mathbf{u}_h\|_U = 0$, $\forall \mathbf{u} \in U$,

HSAS2. from any subsequence $\{\mathbf{u}_{h1}\}_{h\in I}$ of elements $\mathbf{u}_{h1} \in U_{1h}$ which is bounded in U, one can extract a subsequence converging strongly in $(L^2(\Omega))^3$ to an element of U,

HSAS3. $\lim_{h\to 0} \inf_{\mathbf{u}_{0h} \in U_{0h}} \|\mathbf{u}_0 - \mathbf{u}_{0h}\|_U = 0$.

To get meaningful approximations, the sequences of discrete sources have to satisfy:

HSDS1. $\lim h \to 0 \|\mathbf{J}_e - \mathbf{J}_{eh}\|_{0,\Omega} = 0$,

HSDS2. $\lim h \to 0 \|\mathbf{J}_m - \mathbf{J}_{mh}\|_{0,\Omega} = 0$,

HSDS3. $\lim h \to 0 \|\mathbf{f}_R - \mathbf{f}_{Rh}\|_{0,\Gamma} = 0$.

The following is one of the main results of this section:

Theorem 6. *Under the hypotheses HD1–HD3, HM1–HM3, HM7–HM9, HB1, HB3S, HM13–HM15, HSAS1–HSAS3, HSDS1–HSDS3, if HM10 is satisfied by the anisotropic media and HM11 and HM12 are satisfied by the bianisotropic materials involved, then the sequence* $\{\mathbf{E}_h\}$ *of solutions of Problem 3 strongly converges to* $\mathbf{E} \in U$, $\mathbf{E}$ *being the unique solution of Problem 2.*

Proof. The proof is only sketched being analogous to that of Theorem 5.3 of [10]. The first part of the proof shows that, under the indicated hypotheses, for any sufficiently small $h \in I$, we get a unique solution $\mathbf{E}_h$ of Problem 3.

Thus, since the hypotheses guarantee also the well posedness of Problem 2, we can deal, for sufficiently small $h \in I$, with $\mathbf{E}$ and $\mathbf{E}_h$.

The last part of the proof verifies that the sequence $\|\mathbf{E} - \mathbf{E}_h\|_U$ strongly converges to zero. □

The sequence of finite dimensional subspaces for the Galerkin approximation is typically built using the finite element method [29]. This involves the use of a sequence of triangulations $\{\mathcal{T}_h\}$, $h \in I$, of $\overline{\Omega}$ and a specific finite element on each triangulation $\mathcal{T}_h$ [29].

To avoid some technicalities arising with curved boundaries, we assume that [29] (p. 65)

HD4. Ω is a polyhedron (i.e., $\overline{\Omega} = \bigcup_{T \in \mathcal{T}_h} T$).

Edge elements defined on tetrahedra are very often employed for approximating fields belonging to $H(\text{curl}, \Omega)$. For this reason, we assume [29–31]:

HFE1. the family $\{\mathcal{T}_h\}$ of triangulations is regular,

HFE2. $\mathcal{T}_h$ is made up of tetrahedra, $\forall h \in I$,

HFE3. edge elements of a given order defined on tetrahedra are used to build U_h, $\forall h \in I$.

By classical results in finite element theory, we can now conclude that whenever HD1, HD2, HD4, HFE1–HFE3 are satisfied, the space sequence $\{U_h\}$ verifies conditions HSAS1, HSAS2 and HSAS3.

Thus, we obtain the second main results of this section:

Theorem 7. *Under the hypotheses HD1–HD4, HM1–HM3, HM7–HM9, HB1, HB3S, HM13–HM15, HSDS1–HSDS3, HFE1–HFE3, if HM10 is satisfied by the anisotropic media and HM11 and HM12 are satisfied by the bianisotropic materials involved, then Problem 3 is a convergent approximation of Problem 2.*

5. Some Information about the Exploited Finite Element Simulator

In this section, we provide some specific considerations related to the implementation of our finite element code that was used to obtain the numerical solutions to the problems. A first order edge element based Galerkin approach is adopted [32], and most of the details are analogous to the two-dimensional implementation found in [18]. For any mesh adopted, we get the finite dimensional space U_h. In it, we can find the test functions $\mathbf{v}_{hi}$, $i \in \{1, ..., ne\}$, where ne is the number of edges of the mesh. Then, denoting the vector of unknowns as $[e_h] \in \mathbb{C}^{ne}$ and using Equations (7), (18) and (19), we can obtain the following matrix equation:

$$[A_h][e_h] = [l_h]. \tag{22}$$

Here, $[A_h]$ is the complex matrix whose entries are obtained from Equation (7) and are given by:

$$\begin{aligned}[A_h]_{ij} = {} & c_0 \left(Q \,\text{curl}\, \mathbf{v}_{hj}, \text{curl}\, \mathbf{v}_{hi}\right)_{0,\Omega} - \frac{\omega^2}{c_0} \left(P\, \mathbf{v}_{hj}, \mathbf{v}_{hi}\right)_{0,\Omega} - j\omega \left(M\, \mathbf{v}_{hj}, \text{curl}\, \mathbf{v}_{hi}\right)_{0,\Omega} \\ & - j\omega \left(L \,\text{curl}\, \mathbf{v}_{hj}, \mathbf{v}_{hi}\right)_{0,\Omega} + j\omega \left(Y\, (\mathbf{n} \times \mathbf{v}_{hj} \times \mathbf{n}), \mathbf{n} \times \mathbf{v}_{hi} \times \mathbf{n}\right)_{0,\Gamma}, \; i, j = 1, ..., ne. \end{aligned} \tag{23}$$

The entries $[l_h]_i$ are obtained trivially from (18) by replacing $\mathbf{v}$ with $\mathbf{v}_{hi}$. In general, $[A_h]$ is a non-Hermitian complex matrix and in our approach we made use of iterative methods for the solution of the algebraic system. In particular, we exploited the biconjugate gradient method with Jacobi preconditioner [33]. The solution $[e_h]_i$ obtained in the i-th iteration is accepted only when the Euclidean norm of error satisfies $||[A_h][e_h]_i - [l_h]|| < \delta ||[l_h]||$. Here, δ is a fixed value denoting the acceptable tolerance, which is set as $\delta = 10^{-p}$, p being an integer (see Section 5 of [18,33]). For the test problems of Sections 7.3 and 7.4, the value p was set equal to 10 and 5, respectively. The solutions obtained were checked for convergence by refining the mesh until stable results were achieved.

6. Some Hints to Apply the Developed Theory

The developed theory required the introduction of 32 hypotheses: four on the domain (HD1–HD4), four on the boundary conditions (HB1–HB3 and HB3S), 15 on the media involved (and, as it will be shown in Section 7, on the way, they rotate; HM1–HM15), three on the sequence of approximating space (HSAS1–HSAS3), three on the sequence of discrete sources (HSDS1–HSDS3) and three on the finite element discretization (HFE1–HFE3).

The main results of this manuscript, related to the well posedness of the problem of interest and to the convergence of its finite element approximation, make use, respectively, of 17 and 24 of these assumptions.

In order to ease the exploitation of the main outcomes, we observe that most of these hypotheses can be verified immediately for important practical problems. This is true, in particular, for conditions HD1–HD4, HB1–HB3 and HB3S, HM1–HM8, HSDS1–HSDS3, and HFE1–HFE3. Hypotheses HSAS1–HSAS3 are not involved in the indicated theorems. As for the other hypotheses to be verified, in the following, we provide some hints which can be of help to show that assumptions HM9–HM15 holds true.

Let us firstly focus on the additional hypotheses we have introduced to prove condition (10) (that is, HM13 and HM14). In this section, we extensively use the notation introduced in Equation (12) and the line following it.

One simpler way to find the constant involved in hypothesis HM13 is provided by the following Lemma.

Lemma 1. *Suppose that P_{ss} is uniformly positive definite in $\Omega_{el} \subset \Omega$ that is $\exists C_1 > 0$ such that*

$$\int_{\Omega_{el}} \mathbf{u}^* P_{ss} \mathbf{u} \geq C_1 \int_{\Omega el} |\mathbf{u}|^2 = C_1 ||\mathbf{u}||^2_{0,\Omega_{el}} \ \forall \mathbf{u} \in (L^2(\Omega))^3. \tag{24}$$

Whenever $\Omega_{el} = \Omega$, we can simply define $C_{PS} = C_1$.

Whenever Ω_{el} is not the whole Ω, suppose that, in the complementary region, P_s is uniformly positive or negative definite, that is, $\exists C_5 > 0$ such that

$$\left| \int_{\Omega \setminus \Omega_{el}} \mathbf{u}^* P_s \mathbf{u} \right| \geq C_5 ||\mathbf{u}||^2_{0,\Omega \setminus \Omega_{el}}. \tag{25}$$

Whenever $\Omega_{el} = \emptyset$, we simply have $C_{PS} = C_5$ and we can set

$$C_{PS} = \min_{i \in I} \inf_{\mathbf{x} \in \Omega_i} \lambda_{min}(P_s), \tag{26}$$

where λ_{min} denotes the minimum of the magnitudes of the eigenvalues of the Hermitian symmetric matrix P_s.

Finally, whenever Ω_{el} is neither the empty set nor the whole domain, under assumptions HM2 and HM3, condition HM13 is satisfied with C_{PS} given by

$$C_{PS} = \frac{1}{\sqrt{2}} \min \left(\sqrt{(1-\alpha)} C_5, \sqrt{C_1^2 + (1 - \frac{1}{\alpha}) C_3^2} \right), \tag{27}$$

where $C_3 > 0$ is defined by

$$\left| \int_{\Omega_{el}} \mathbf{u}^* P_s \mathbf{u} \right| \leq C_3 \|\mathbf{u}\|^2_{0,\Omega_{el}} \tag{28}$$

and α is such that $1 > \alpha > \frac{C_3^2}{C_1^2 + C_3^2} > 0$.

Lemma 1 is proved in the Appendix A by using a technique developed in [34].

In an analogous way, by replacing P with Q in Equations (24), (25) and (28) , we define, respectively, Ω_{ml} and the constants $C_2 > 0$, $C_4 > 0$ and $C_6 > 0$ and deduce that condition HM14 is satisfied if we set

$$C_{QS} = \min_{i \in I} \inf_{\mathbf{x} \in \Omega_i} \lambda_{min}(Q_s), \tag{29}$$

whenever $\Omega_{ml} = \emptyset$, $C_{QS} = C_2$ whenever $\Omega_{ml} = \Omega$ or

$$C_{QS} = \frac{1}{\sqrt{2}} \min \left(\sqrt{(1-\alpha)} C_6, \sqrt{C_2^2 + (1 - \frac{1}{\alpha}) C_4^2} \right), \tag{30}$$

being α such that $1 > \alpha > \frac{C_4^2}{C_2^2 + C_4^2} > 0$, when $\Omega_{ml} \neq \Omega$ and $\Omega_{ml} \neq \emptyset$.

The above lemma will be heavily exploited to show the applicability of our theory to many practical problems of interest. However, it does not imply that it is not possible to find larger values of C_{PS}. For example, whenever P_s is uniformly definite in Ω that is $\exists C_7 > 0$ such that

$$\left| \int_\Omega \mathbf{u}^* P_s \mathbf{u} \right| \geq C_7 ||\mathbf{u}||^2_{0,\Omega}, \tag{31}$$

we can choose for C_{PS} the largest between C_7 and the value obtained by using Lemma 1.

This is of interest in order to reduce the restrictions due to inequality HM15. In order to check its validity, we also have to evaluate the continuity constants $C_L > 0$ and $C_M > 0$. From their very definitions, one can estimate these values and set for example

$$C_L = \max_{i \in I_b} \sup_{\mathbf{x} \in \Omega_i} \sqrt{\lambda_{max}(L^* L)} \tag{32}$$

and

$$C_M = \max_{i \in I_b} \sup_{\mathbf{x} \in \Omega_i} \sqrt{\lambda_{max}(M^* M)}, \tag{33}$$

where λ_{max} denotes the maximum of the magnitudes of the eigenvalues of the Hermitian symmetric matrix to which it applies.

We now look for simple techniques to check the validity of hypotheses HM9–HM12. Our previous considerations assume that we know the constitutive matrices P, Q, L and M. The next ones, on the contrary, are based on κ, ν, χ and γ. In order to deduce this form of the constitutive parameters, one can use the equations reported below Equation (14) under hypothesis HM7.

To check the validity of assumptions HM9–HM12, the constants $C_{\kappa,d}$, $C_{\nu,d}$, $C_{\kappa,r}$, $C_{\nu,r}$, $C_{\kappa,s}$ and $C_{\nu,s}$ have to be evaluated (see Remark 1). For $C_{\kappa,d}$, $C_{\nu,d}$, $C_{\kappa,s}$ and $C_{\nu,s}$ one has simply to apply the definitions, for example by calculating

$$C_{\kappa,d} = \min_{i \in I} \inf_{\mathbf{x} \in \Omega_i} |determinant(\kappa)|, \tag{34}$$

$$C_{\nu,d} = \min_{i \in I} \inf_{\mathbf{x} \in \Omega_i} |determinant(\nu)|, \tag{35}$$

$$C_{\kappa,s} = \max_{i \in I} \sup_{\mathbf{x} \in \Omega_i} \left((\sum_{i,j=1}^{3} |\kappa_{ij}|) - \min_{i=1,2,3} |\kappa_{ii}| \right), \tag{36}$$

$$C_{\nu,s} = \max_{i \in I} \sup_{\mathbf{x} \in \Omega_i} \left((\sum_{i,j=1}^{3} |\nu_{ij}|) - \min_{i=1,2,3} |\nu_{ii}| \right). \tag{37}$$

As for $C_{\kappa,r}$ and $C_{\nu,r}$ the following consideration might be helpful. By definition

$$C_{\kappa,r} = \min_{i \in I} \inf_{\mathbf{x} \in \Omega_i} \min_{\mathbf{l}_{1,3,n} \in \mathbb{R}^3 : \|\mathbf{l}_{1,3,n}\|_2 = 1} \sqrt{\left(\mathbf{l}_{1,3,n}^T \kappa_{is} \mathbf{l}_{1,3,n} \right)^2 + \left(\mathbf{l}_{1,3,n}^T \kappa_{iss} \mathbf{l}_{1,3,n} \right)^2}, \tag{38}$$

$$C_{\nu,r} = \min_{i\in I} \inf_{\mathbf{x}\in\Omega_i} \min_{\mathbf{l}_{1,3,n}\in\mathbb{R}^3:\|\mathbf{l}_{1,3,n}\|_2=1} \sqrt{\left(\mathbf{l}_{1,3,n}^T \nu_{is} \mathbf{l}_{1,3,n}\right)^2 + \left(\mathbf{l}_{1,3,n}^T \nu_{iss} \mathbf{l}_{1,3,n}\right)^2}, \tag{39}$$

where κ_{is} and κ_{iss} are the symmetric matrices obtained by the usual decomposition of κ^{-1} and similarly ν_{is} and ν_{iss} are those corresponding to ν^{-1}. If both the symmetric matrices involved in the above expressions are semi-definite, then we can deduce the following lower bounds:

$$C_{\kappa,r} = \min_{i\in I} \inf_{\mathbf{x}\in\Omega_i} \sqrt{\left(\lambda_{min}(\kappa_{is})\right)^2 + \left(\lambda_{min}(\kappa_{iss})\right)^2}, \tag{40}$$

$$C_{\nu,r} = \min_{i\in I} \inf_{\mathbf{x}\in\Omega_i} \sqrt{\left(\lambda_{min}(\nu_{is})\right)^2 + \left(\lambda_{min}(\nu_{iss})\right)^2}. \tag{41}$$

If we also define

$$C_{\chi,s} = \max_{i\in I} \sup_{\mathbf{x}\in\Omega_i} \left(\left(\sum_{i,j=1}^{3} |\chi_{ij}| \right) - \min_{i=1,2,3} |\chi_{ii}| \right), \tag{42}$$

$$C_{\gamma,s} = \max_{i\in I} \sup_{\mathbf{x}\in\Omega_i} \left(\left(\sum_{i,j=1}^{3} |\gamma_{ij}| \right) - \min_{i=1,2,3} |\gamma_{ii}| \right), \tag{43}$$

the sufficient condition for the regularity used for proving uniqueness can be expressed as

$$K_u = \frac{4 C_{\chi,s} C_{\gamma,s}}{\left(-C_{\kappa,s} + \sqrt{C_{\kappa,s}^2 + 4 C_{\kappa,d} C_{\kappa,r}}\right)\left(-C_{\nu,s} + \sqrt{C_{\nu,s}^2 + 4 C_{\nu,d} C_{\nu,r}}\right)} < 1. \tag{44}$$

7. Implications for Rotating Axisymmetric Objects

In this section, we show the implications of the developed theory for three-dimensional problems involving rotating axisymmetric objects.

The class of scattering problems of interest involves rotating axisymmetric objects illuminated by time-harmonic electromagnetic fields. Even though our theory does not limit the number of objects involved, in this section, we show the results computed in the presence of just one rotating rigid body (with angular velocity ω_s) because, on the one hand, this is enough to get bianisotropic effects and, on the other hand, notwithstanding the limitation, it is still possible to define problems whose solutions, to the best of the authors' knowledge, is not known. In these cases, our solutions may then be considered as benchmarks.

By the same token, it is not necessary to consider very complicated configurations of materials. This is the reason why in this subsection we analyze problems involving objects rotating in vacuum. In our notation, the empty space is characterized by $P = c_0\varepsilon_0 I_3$, $Q = \frac{1}{c_0\mu_0} I_3$, $L = M = 0$, being I_3 the identity matrix. In order to avoid problems with convective currents, which can become surface currents [35], we assume that all rotating media in their rest frames have the electric conductivity $\sigma = 0$ and real-valued ε and μ. However, we need to know the constitutive parameters when the media are rotating. To get these results, we recall that for media in motion with a generic velocity field $\mathbf{v}$ we have [19] (p. 958)

$$\mathbf{D} + \frac{1}{c_0^2}\mathbf{v}\times\mathbf{H} = \varepsilon\left(\mathbf{E} + \mathbf{v}\times\mathbf{B}\right), \tag{45}$$

$$\mathbf{B} - \frac{1}{c_0^2}\mathbf{v}\times\mathbf{E} = \mu\left(\mathbf{H} - \mathbf{v}\times\mathbf{D}\right). \tag{46}$$

If $\mu \neq 0$, from Equation (46), one immediately gets

$$\mathbf{H} = \frac{1}{\mu}\mathbf{B} - \frac{1}{\mu c_0^2}\left(\mathbf{v}\times\mathbf{E}\right) + \left(\mathbf{v}\times\mathbf{D}\right), \tag{47}$$

and, by substituting it in Equation (45), one easily deduces

$$\mathbf{D} - \frac{1}{c_0^2}(\mathbf{v} \times \mathbf{D}) \times \mathbf{v} = \varepsilon \mathbf{E} - \frac{1}{\mu c_0^4}(\mathbf{v} \times \mathbf{E}) \times \mathbf{v} + \frac{\mu_r \varepsilon_r - 1}{\mu c_0^2}(\mathbf{v} \times \mathbf{B}). \tag{48}$$

Cross multiplying (on the left) this equation by $\frac{\mathbf{v}}{v^2}$, being $v = |\mathbf{v}|$, one obtains

$$(\mathbf{v} \times \mathbf{D}) = \frac{\mu_r \varepsilon_r c_0^2 - v^2}{\mu c_0^2 (c_0^2 - v^2)}(\mathbf{v} \times \mathbf{E}) - \frac{1}{\mu}\frac{\mu_r \varepsilon_r - 1}{c_0^2 - v^2}(\mathbf{v} \times \mathbf{B}) \times \mathbf{v} \tag{49}$$

and, by substituting it in the expression of $\mathbf{H}$, one gets [36]

$$\mathbf{H} = \frac{\mu_r \varepsilon_r - 1}{\mu(c_0^2 - v^2)}(\mathbf{v} \times \mathbf{E}) + \frac{1}{\mu}\mathbf{B} - \frac{\mu_r \varepsilon_r - 1}{\mu(c_0^2 - v^2)}(\mathbf{v} \times \mathbf{B}) \times \mathbf{v}. \tag{50}$$

Finally, if one obtains $(\mathbf{v} \times \mathbf{D}) \times \mathbf{v}$ from Equation (49) and substitutes the result in Equation (48), the following expression is obtained:

$$\mathbf{D} = \varepsilon \mathbf{E} + \frac{\mu_r \varepsilon_r - 1}{\mu c_0^2 (c_0^2 - v^2)}(\mathbf{v} \times \mathbf{E}) \times \mathbf{v} + \frac{\mu_r \varepsilon_r - 1}{\mu(c_0^2 - v^2)}(\mathbf{v} \times \mathbf{B}). \tag{51}$$

The last two equations allow us to find the constitutive parameters of the rotating media as perceived in the laboratory frame. Without loss of generality, we can assume that z is the axis of rotation of the rigid body. Then, the velocity field is along the azimuthal direction and has a magnitude given by the constant angular velocity ω_s multiplied by the distance of the considered point from the z axis. In the chosen Cartesian reference frame, one immediately gets $\mathbf{v} = \omega_s(x\hat{\mathbf{y}} - y\hat{\mathbf{x}})$. Then, for a generic vector $\mathbf{A}$, one deduces $\mathbf{v} \times \mathbf{A} = \omega_s x A_z \hat{\mathbf{x}} + \omega_s y A_z \hat{\mathbf{y}} - \omega_s(xA_x + yA_y)\hat{\mathbf{z}}$ and $(\mathbf{v} \times \mathbf{A}) \times \mathbf{v} = \omega_s^2(x^2 A_x + xyA_y)\hat{\mathbf{x}} + \omega_s^2(xyA_x + y^2 A_y)\hat{\mathbf{y}} + \omega_s^2 A_z(x^2 + y^2)\hat{\mathbf{z}}$. By using these expressions in Equations (50) and (51), after simple calculations, one finds the following explicit expressions of the constitutive matrices P, Q, L and M [36]

$$P = a_1 I_3 + b_1 T_1, \tag{52}$$

$$Q = a_2 I_3 - b_1 T_1, \tag{53}$$

$$L = M = \frac{c_0 b_1}{\omega_s} T_2, \tag{54}$$

where $a_1 = \varepsilon_0 \varepsilon_r c_0$, $a_2 = \frac{1}{\mu_0 \mu_r c_0}$, b_1 is the field $\frac{\omega_s^2(\epsilon_r \mu_r - 1)}{\mu_0 \mu_r c_0 (c_0^2 - \omega_s^2(x^2+y^2))}$,

$$T_1 = \begin{bmatrix} x^2 & xy & 0 \\ xy & y^2 & 0 \\ 0 & 0 & x^2 + y^2 \end{bmatrix}, \tag{55}$$

and

$$T_2 = \begin{bmatrix} 0 & 0 & x \\ 0 & 0 & y \\ -x & -y & 0 \end{bmatrix}. \tag{56}$$

Now, we may apply the theory developed in the previous sections to check when these problems are well posed.

7.1. Checking Condition (9) for Problems Involving Rotating Objects

Rotating objects are of particular interest for scattering problems. For this class of problems, it is usual to have absorbing boundary conditions, so that HB3S is satisfied in any case.

To verify conditions HM9–HM12, we calculate κ, χ, γ and ν of the scatterer by using the equations reported below Equation (14). We get:

$$\kappa = c_0 P^{-1} = \frac{c_0}{a_1 + b_1(x^2+y^2)} I + \frac{c_0}{a_1 + b_1(x^2+y^2)} \frac{b_1}{a_1} [(x^2+y^2)I - T_1], \tag{57}$$

$$\chi = -\frac{c_0}{a_1 + b_1(x^2+y^2)} \frac{c_0 b_1}{\omega_s} T_2, \tag{58}$$

$$\gamma = -\chi, \tag{59}$$

$$\nu = a_1 a_2 \kappa. \tag{60}$$

Now, we proceed as indicated in the second part of Section 6 (the one relative to the check of conditions HM9–HM12). In particular, we start calculating the determinant of κ and ν in the scatterer

$$determinant(\kappa) = \frac{c_0^3}{a_1(a_1 + b_1(x^2+y^2))^2}, \tag{61}$$

$$determinant(\nu) = \frac{a_1^3 a_2^3 c_0^3}{a_1(a_1 + b_1(x^2+y^2))^2}. \tag{62}$$

Since in vacuum $\kappa = \frac{1}{\varepsilon_0} I$ and $\nu = \frac{1}{\mu_0} I$, the above determinants reduces respectively to $\frac{1}{\varepsilon_0^3}$ and $\frac{1}{\mu_0^3}$. In order to simplify the analysis and consider the most interesting cases, we restrict our analysis to scatterers made up of homogeneous non-magnetic materials ($\mu_r = 1$) having $\varepsilon_r > 1$. Under this condition in the scatterer, we have $b_1 > 0$ and then $a_1(a_1 + b_1(x^2+y^2))^2 > a_1^3$, so that $determinant(\kappa) < \frac{c_0^3}{a_1^3} = \frac{1}{\varepsilon_0^3 \varepsilon_r^3} < \frac{1}{\varepsilon_0^3}$ and $determinant(\nu) < a_2^3 c_0^3 = \frac{1}{\mu_0^3}$. Thus, by using Equations (34) and (35), the constants $C_{\kappa,d}$ and $C_{\nu,d}$ can be determined by finding the smallest values of the determinants in the scatterer, which is found when the field $b_1(x^2+y^2)$ gets its largest value. Since $b_1(x^2+y^2)$ is an increasing function of x^2+y^2, we finally get

$$C_{\kappa,d} = \frac{c_0^3}{a_1(a_1 + b_{1,max} R^2)^2} \tag{63}$$

and

$$C_{\nu,d} = \frac{c_0^3 a_1^2 a_2^3}{(a_1 + b_{1,max} R^2)^2}, \tag{64}$$

where R is the largest distance of the boundary of the scatterer from its axis of rotation and $b_{1,max}$ is the value which the field b_1 gets for this value of x^2+y^2:

$$b_{1,max} = \frac{\omega_s^2(\varepsilon_r - 1)}{\mu_0 c_0 (c_0^2 - \omega_s^2 R^2)}. \tag{65}$$

For problems involving objects in motion, it is usual practice to introduce the maximum normalized velocity $\beta = \frac{\omega_s R}{c_0} < 1$. In terms of β, we get $b_{1,max} R^2 = \frac{(\varepsilon_r - 1)\beta^2}{\mu_0 c_0 (1-\beta^2)}$ and then

$$C_{\kappa,d} = \frac{(1-\beta^2)^2}{\varepsilon_0^3 \varepsilon_r (\varepsilon_r - \beta^2)^2} \tag{66}$$

and

$$C_{\nu,d} = \frac{\varepsilon_r^2(1-\beta^2)^2}{\mu_0^3(\varepsilon_r-\beta^2)^2}. \tag{67}$$

If now we look for the constants $C_{\kappa,r}$ and $C_{\nu,r}$, we observe that $\kappa^{-1} = \frac{1}{c_0}P$ everywhere while $\nu^{-1} = (a_1a_2\kappa)^{-1} = \frac{1}{a_1a_2c_0}P$ in the scatterer and $\nu^{-1} = \mu_0 I$ in vacuum. Moreover, P is a real symmetric positive definite matrix, both inside and outside the scatterer, and we can use Equations (40) and (41) with $\kappa_{iss} = 0$ and $\nu_{iss} = 0$. Finally, the eigenvalues of P are a_1 and $a_1 + b_1(x^2+y^2)$ in the scatterer and $c_0\varepsilon_0$ in vacuum. Thus, the minimum of the infimum of the λ_{min} involved in those expressions is achieved in both cases in vacuum and we get

$$C_{\kappa,r} = \varepsilon_0, \tag{68}$$

and

$$C_{\nu,r} = \mu_0. \tag{69}$$

Moreover, $C_{\kappa,s}$ can be deduced by computing the suprema reported in Equation (36), inside and outside the scatterer. After some calculation, one can find that inside the scatterer the supremum is equal to $\frac{2}{\varepsilon_0\varepsilon_r}$ and outside it is $\frac{2}{\varepsilon_0}$, so that

$$C_{\kappa,s} = \frac{2}{\varepsilon_0}. \tag{70}$$

In an analogous way, we get

$$C_{\nu,s} = \frac{2}{\mu_0}. \tag{71}$$

Finally, by using Equations (58) and (59), we get that the suprema reported in Equations (42) and (43) are equal to zero outside of the scatterer and strictly positive inside it. After a few calculations, we get such strictly positive quantities

$$C_{\gamma,s} = C_{\chi,s} = \frac{2\sqrt{2}c_0^2 b_{1,max}R}{\omega_s(a_1 + b_{1,max}R^2)} = \frac{2\sqrt{2}c_0^2(\varepsilon_r-1)\beta}{\varepsilon_r-\beta^2}. \tag{72}$$

Now, to satisfy condition (9), we can substitute the previous expressions of $C_{\kappa,d}$, $C_{\nu,d}$, $C_{\kappa,r}$, $C_{\nu,r}$, $C_{\kappa,s}$, $C_{\nu,s}$, $C_{\gamma,s}$ and $C_{\chi,s}$. We get

$$\begin{aligned} 1 > K_u &= \frac{4C_{\chi,s}C_{\gamma,s}}{\left(-C_{\kappa,s}+\sqrt{C_{\kappa,s}^2+4C_{\kappa,d}C_{\kappa,r}}\right)\left(-C_{\nu,s}+\sqrt{C_{\nu,s}^2+4C_{\nu,d}C_{\nu,r}}\right)} = \\ &= \frac{32\varepsilon_r(\varepsilon_r-1)^2\beta^2}{\left(-2\varepsilon_r(\varepsilon_r-\beta^2)+2\sqrt{\varepsilon_r^4+\varepsilon_r+\beta^4\varepsilon_r(\varepsilon_r+1)-2\beta^2\varepsilon_r(\varepsilon_r^2+1)}\right)} \cdot \\ &\cdot \frac{1}{\left(-2(\varepsilon_r-\beta^2)+2\sqrt{2\varepsilon_r^2+\beta^4(\varepsilon_r^2+1)-2\beta^2\varepsilon_r(\varepsilon_r+1)}\right)}. \end{aligned} \tag{73}$$

In Figure 1, K_u is plotted with respect to β, with ε_r as a parameter. It shows that the range $[0, \beta_{\text{critical}}]$ of β for which the validity of condition (9) is guaranteed becomes larger and larger as ε_r gets smaller and smaller, as expected. However, our analysis provides quantitative results on such a range. As it is easy to check, it is so large that no significant restriction on β emerges for practical applications.

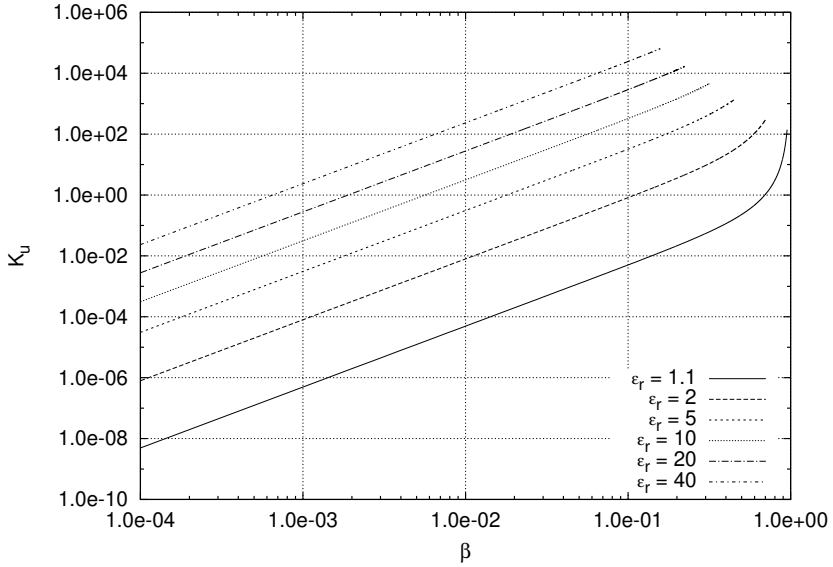

Figure 1. Plot of K_u versus β for rotating axisymmetric objects. The plots are shown for various values of ε_r. Condition (9) is satisfied for $K_u < 1$.

The plot of β_{critical} is shown, together with another significant threshold value obtained in the next subsection, in Figure 2.

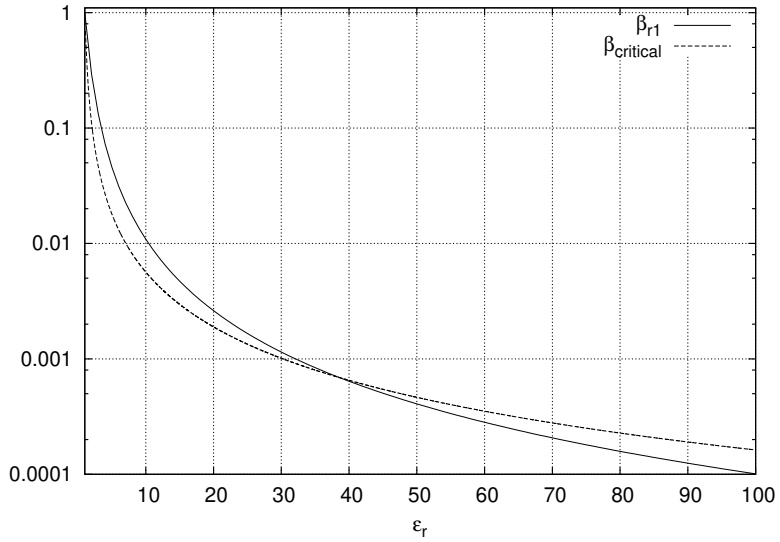

Figure 2. Behaviours of β_{r1} and β_{critical} versus ε_r. β_{critical} is the upper bound on β required to satisfy condition (9) while β_{r1} is that required for condition (10).

7.2. Checking Conditions (10) for Problems Involving Rotating Objects

In this section, we examine the situations in which condition (10) holds true for the class of problems considered. By definition, inside and outside the scatterer, we get $P_s = P$, $P_{ss} = 0$, $Q_s = Q$, $Q_{ss} = 0$. In order to check the indicated condition, we need to find the constants C_{PS}, C_{QS}, C_L and C_M. As for C_L and C_M, by using Equations (32) and (33), we have to evaluate the suprema involved just inside the scatterer. Since $M = L$, we can focus just on one of the two constants. The eigenvalues of L^*L are found to be 0 and $\left(\frac{c_0 b_1}{\omega_s}\right)^2 (x^2 + y^2)$ (with multiplicity 2). As already pointed out, in the

following, in order to simplify the analysis, we assume that the scatterer medium is characterized by $\varepsilon_r > 1$ and $\mu_r = 1$ in its rest frame. Under this hypothesis, the field b_1 is strictly positive and then

$$C_L = C_M = b_{1,max}\frac{c_0 R}{\omega_s}. \tag{74}$$

We already know that inside the scatterer the eigenvalues of P_s are $a_1 = \varepsilon_0\varepsilon_r c_0$ and $a_1 + b_1(x^2 + y^2)$ while outside it we have $P_s = c_0\varepsilon_0 I_3$. Under the indicated hypotheses for the scatterer medium, since $\Omega_{el} = \emptyset$, from Lemma 1 (see Equation (26)), we trivially get that HM13 is satisfied with

$$C_{PS} = \varepsilon_0 c_0. \tag{75}$$

Similarly, the eigenvalues of Q_s inside the scatterer are $a_2 = \frac{1}{c_0\mu_0\mu_r} = \frac{1}{c_0\mu_0}$ and $a_2 - b_1(x^2 + y^2)$ while outside the rotating object we have $Q_s = \frac{1}{c_0\mu_0} I_3$. Since $\Omega_{ml} = \emptyset$ by Equation (29), we obtain

$$C_{QS} = a_2 - b_{1,max}R^2, \tag{76}$$

which is positive when $\beta < \frac{1}{\sqrt{\varepsilon_r}}$. Under this condition, HM14 is satisfied as well.

By using Equations (74)–(76), the crucial inequality which is present in assumption HM15 reads

$$C_{QS} - \frac{C_L C_M}{C_{PS}} = a_2 - b_{1,max}R^2 - b_{1,max}^2\frac{c_0 R^2}{\varepsilon_0\omega_s^2} > 0. \tag{77}$$

After the substitution of a_2 and $b_{1,max}$, it can be shown to be equivalent to the following:

$$1 + \beta^2(\varepsilon_r - 2 + \varepsilon_r^2) + \beta^4\varepsilon_r > 0. \tag{78}$$

The left-hand side in inequality (78) is a parabola in terms of β^2. We can find two roots β_{r1}^2, β_{r2}^2 given by

$$\begin{cases} \beta_{r1}^2 = \frac{\varepsilon_r^2+2-\varepsilon_r-\sqrt{(\varepsilon_r^2+2-\varepsilon_r)^2-4\varepsilon_r}}{2\varepsilon_r} = \frac{\varepsilon_r^2+2-\varepsilon_r-(\varepsilon_r-1)\sqrt{\varepsilon_r^2+4}}{2\varepsilon_r} \\ \beta_{r2}^2 = \frac{\varepsilon_r^2+2-\varepsilon_r+\sqrt{(\varepsilon_r^2+2-\varepsilon_r)^2-4\varepsilon_r}}{2\varepsilon_r} = \frac{\varepsilon_r^2+2-\varepsilon_r+(\varepsilon_r-1)\sqrt{\varepsilon_r^2+4}}{2\varepsilon_r} \end{cases} \tag{79}$$

which are both real numbers. Such numbers are positive because the parabola becomes larger and larger for $\beta \to \infty$ and is equal to 1 and has a negative derivative (equal to $\varepsilon_r - 2 - \varepsilon_r^2$) when $\beta = 0$.

In particular, we have that

$$\beta_{r1}^2 < \frac{1}{\varepsilon_r} < 1, \tag{80}$$

since $\beta_{r1}^2 - \frac{1}{\varepsilon_r} = \frac{(\varepsilon_r-1)(\varepsilon_r-\sqrt{\varepsilon_r^2+4})}{2\varepsilon_r} < 0$ and $\beta_{r2}^2 > 1$ because $\beta_{r2}^2 - 1 = \frac{(\varepsilon_r-1)(\varepsilon_r-2+\sqrt{\varepsilon_r^2+4})}{2\varepsilon_r} > 0$.

Since a value greater than one is not possible for β, condition HM15 can only be satisfied for β in the range $[0, \beta_{r1}]$. In the same range of β condition, HM14 is a priori satisfied (see Equation (80) and the comment after Equation (76)) and then (10) does hold true.

The behaviours of β_{r1} and β_{critical} versus ε_r are shown in Figure 2. In order to satisfy conditions (9) and (10) and then to obtain the well posedness of the problem, β should be smaller than the smallest of β_{r1} and β_{critical}. The two plots in Figure 2 cross at about $\varepsilon_r \simeq 38.5$ and for smaller (respectively, larger) values the stronger condition on β is given by condition (9) (respectively, (10)).

7.3. Application to Rotating Sphere

In this subsection, we apply the theory to a specific case: a rotating sphere of radius R_s is illuminated by a linearly polarized plane wave propagating along the x-axis. A first order approximation of the solution of this problem is given by the semi-analytic procedure discussed by De Zutter in [1].

Our formulation of the problem requires the definition of a bounded domain Ω, which is taken as a sphere of radius R_d. The boundary conditions we enforce on Γ have Y equal to the admittance of vacuum and are inhomogeneous ($\mathbf{f}_R \neq 0$), to take account of the incident field.

The parameters considered are $\varepsilon_r = 8$, $\mu_r = 1$, $R_s = 1$ m, $R_d = 4$ m. The incident plane wave has a frequency of 50 MHz and an amplitude of the electric field of 1 V/m.

In order to analyze significant test cases for our theory and, at the same time, show its generality, we consider exceptionally large rotational speeds, without worrying about the mechanical stability of the rigid body. The rotating speed we consider is $\omega_s = 8.0\ 10^{-3} c_0$ rad/s, which corresponds to a maximum normalized velocity of $\beta = 8.0\ 10^{-3}$. This is within the limits of applicability of our theory since for $\varepsilon_r = 8$ we get $\beta_{r1} = 1.728 \times 10^{-2}$ and $\beta_{critical} = 8.124 \times 10^{-3}$. The above qualitative considerations, which apply also to the next test case (see Subsection 7.4), justify the simplified approach we have adopted (see Remark 1).

A comparison of the first order edge element based Galerkin finite element solution against the De Zutter semi-analytic procedure is carried out when the incident field is polarized along the z-axis and the spherical domain is discretized rather uniformly with a mesh having 475,797 nodes and 2,496,192 tetrahedra.

All values of the significant quantities defining our model are reported in Table 1. It includes also the parameters defining the model considered in the next subsection.

Table 1. Values of the parameters defining our models.

Type of Problem	Radius of the Domain	Geometrical Parameters of the Scatterers	Incident Plane Wave	Scatterers Constitutive Parameters	Maxima of the Normalized Velocity	Mesh of Tetrahedra
rotating sphere	4 m	$R_s = 1$ m	$f = 50$ MHz, $\|\mathbf{E}\| = 1$ V/m, propagation axis: x, polarization: linear, z	$\sigma = 0$, $\varepsilon_r = 8$, $\mu_r = 1$	$\beta = 8\ 10^{-3}$	475,797 nodes, 2,496,192 elements
rotating torus	2 m	$R = 0.15$ m, $r = 0.15$ m	$f = 500$ MHz, $\|\mathbf{E}\| = 1$ V/m, propagation axis: x, polarization: linear, z	$\sigma = 0$, $\varepsilon_r = 20$, $\mu_r = 1$	$\beta = 1.8\ 10^{-3}$	36,993 nodes, 2,192,940 elements

Figures 3 and 4 show, respectively, the magnitude and phase of the components of the electric field evaluated along a circle in the xz plane, which is centered at the origin and has a radius of 1.5 m. The results obtained from the finite element solver are compared with the semi-analytical solution obtained using the De Zutter procedure [1]. All three components are in very good agreement. Due to the well posedness and the finite element approximability of the problem, this shows that the De Zutter first order (in β) approximation provides reliable results even for very large rotational speeds.

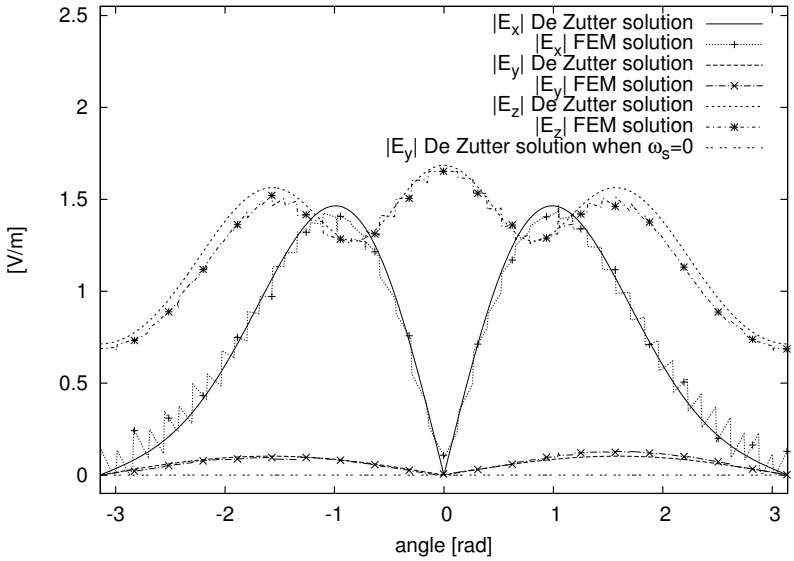

Figure 3. Comparison of the magnitudes of the electric field components along a circle in the xz plane at 1.5 m from the center of the rotating sphere. The horizontal axis represents the angle measured in radians from the x-axis.

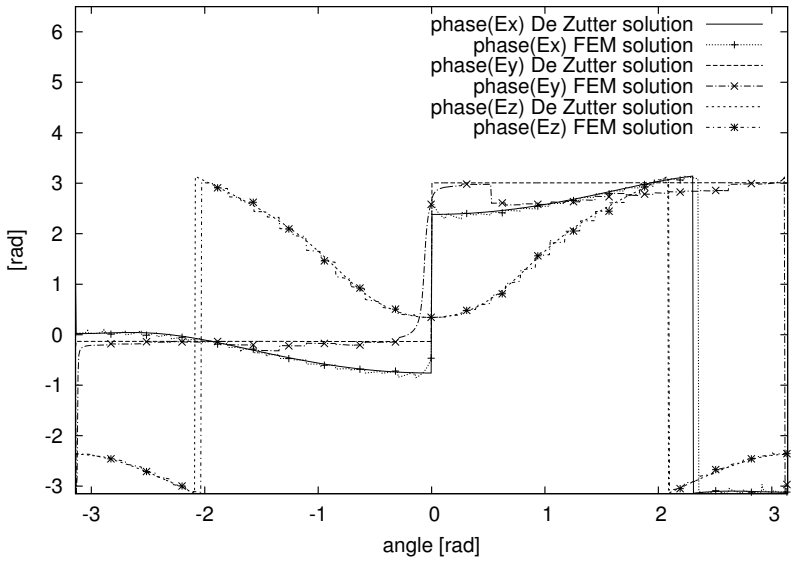

Figure 4. Comparison of the phases of the electric field components along a circle in xz plane at 1.5 m from the center of the rotating sphere. The horizontal axis represents the angle measured in radians from the x-axis.

In particular, we can observe that the y-component of the field is purely a result of rotation. This component amounts to 10 percent of the incident field. These kinds of effects on the fields can be particularly important for inverse problems to figure out the rotational speeds, for example, by extending the algorithms discussed in [37,38].

The same sort of agreement between the two solutions is further confirmed by the fields along similar circles on other planes or along lines parallel to coordinate axes, for different polarizations and directions of propagation of the illuminating field.

For example, Figures 5 and 6 show the magnitude and phase of the z component of electric field along the y-axis. Along this line, the motion of the sphere causes a difference in magnitude of up to 20 percent of the incident field.

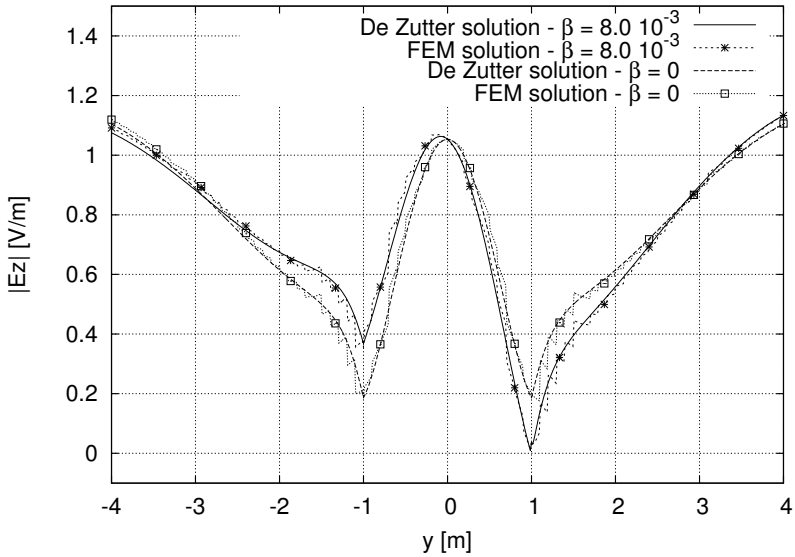

Figure 5. Comparison of the magnitudes of the z-component of the electric field along the y-axis for the rotating sphere.

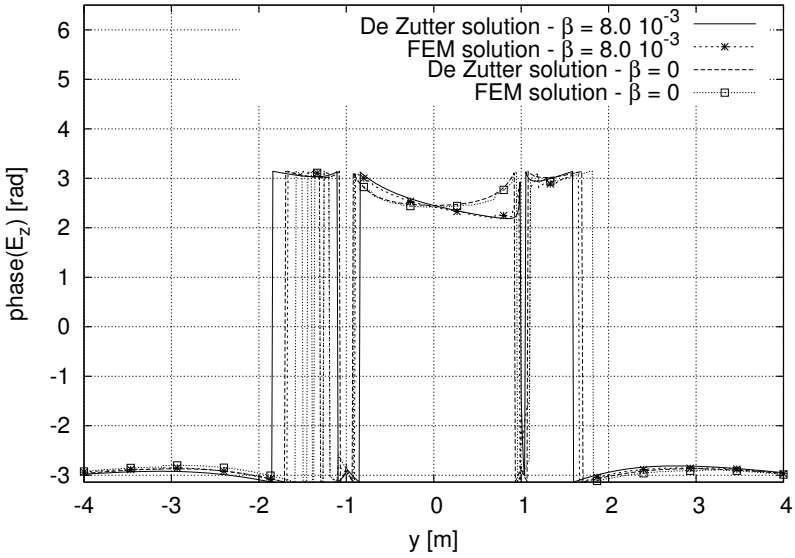

Figure 6. Comparison of the phases of the z-component of the electric field along the y-axis for the rotating sphere.

7.4. Application to Rotating Torus

Thus far, we have considered problems for which a semi-analytic solution is available. In order to illustrate the full relevance of the new results, we now tackle problems for which no solution can be found in the open literature, to the best of the authors' knowledge.

For this, let us consider a homogeneous torus rotating about its axis. The geometry of the problem is described in Figure 7.

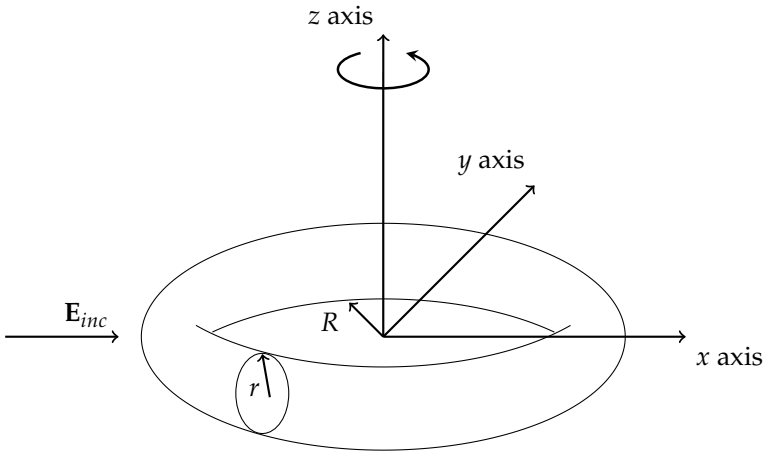

Figure 7. Geometry of the toroidal scatterer. The toroid rotates about the z-axis with angular velocity ω_s. R and r are as shown in the figure and are respectively the "major radius" and the "minor radius" of the torus.

The value of both radii (R and r) is 0.15 m. The torus is made of a material with $\varepsilon_r = 20$. The domain of numerical investigation is a sphere of radius 2 m. We consider a plane wave incident along the x-axis with the electric field polarized along the z-axis and with magnitude 1 V/m and frequency $f = 500$ MHz. For $\varepsilon_r = 20$, the upper bounds for β allowing the application of our theory are given by $\beta_{r1} = 2.618 \times 10^{-3}$ and $\beta_{critical} = 1.893 \times 10^{-3}$. Respecting these limits lets us consider values of $\omega_s \leq 4.0 \times 10^{-3} c_0$ rad/s, which corresponds to a maximum β value of 1.8×10^{-3}.

The first order edge element based Galerkin finite element solution we show in the following is obtained with a three-dimensional tetrahedral mesh having 2,192,940 elements and 36,993 nodes.

To gain an understanding of the solution, we may consider the behaviours of the field along the three coordinate directions for different rotating speed values. Here, we consider ω_s in the set $\{0, 1.0 \times 10^{-3} c_0, 2.0 \times 10^{-3} c_0, 4.0 \times 10^{-3} c_0\}$. The electric field components along the x-axis are shown in Figure 8.

In this case, the largest effect due to motion occurs in the z component of the field, where a difference as large as twice the incident field can be observed between the cases with $\omega_s = 0$ and $\omega_s = 4.0 \times 10^{-3} c_0$. For the other two speeds considered, the effects are smaller but still discernible. There are effects also on the components $|E_x|$ and $|E_y|$ along the x-axis, the maximum difference from the stationary solution being around twice the incident field in the former case and fifty percent of the incident field in the latter one. The norm of the total field $|\mathbf{E}|$ is dominated by the z-component and hence both of them carry roughly the same information when plotted along the x-axis. Along the y-axis for $\omega_s = 4.0 \times 10^{-3} c_0$, the differences from the stationary case are as large as twice the incident field for $|E_x|$, fifty percent of incident field for $|E_y|$ and three times for $|E_z|$. This is shown in Figure 9.

In this case, the total field $|\mathbf{E}|$ is also largely similar to the z component and the difference from the stationary solution is about three times the incident field. For the other speeds considered, the rotational effects on the fields are quite small along this direction. Finally, we do not show the behaviour of the electric field along the z-axis because, in this case, the effects due to motion for all the components are quite small (less than 2 percent) for the speeds considered.

Hence, we can conclude that in this case the fields along x- and y -directions carry significant information about the rotating speed of the toroidal scatterer.

As previously mentioned, the changes in the fields induced by the motion are important because it may be useful for the reconstruction of the velocity profiles of rotating objects. This could be of interest, for example, for rotating celestial bodies. Moreover, since our theory guarantees the well posedness of the problems and the convergence of the numerical solutions, the presented results can be considered as benchmarks for other approaches or numerical techniques.

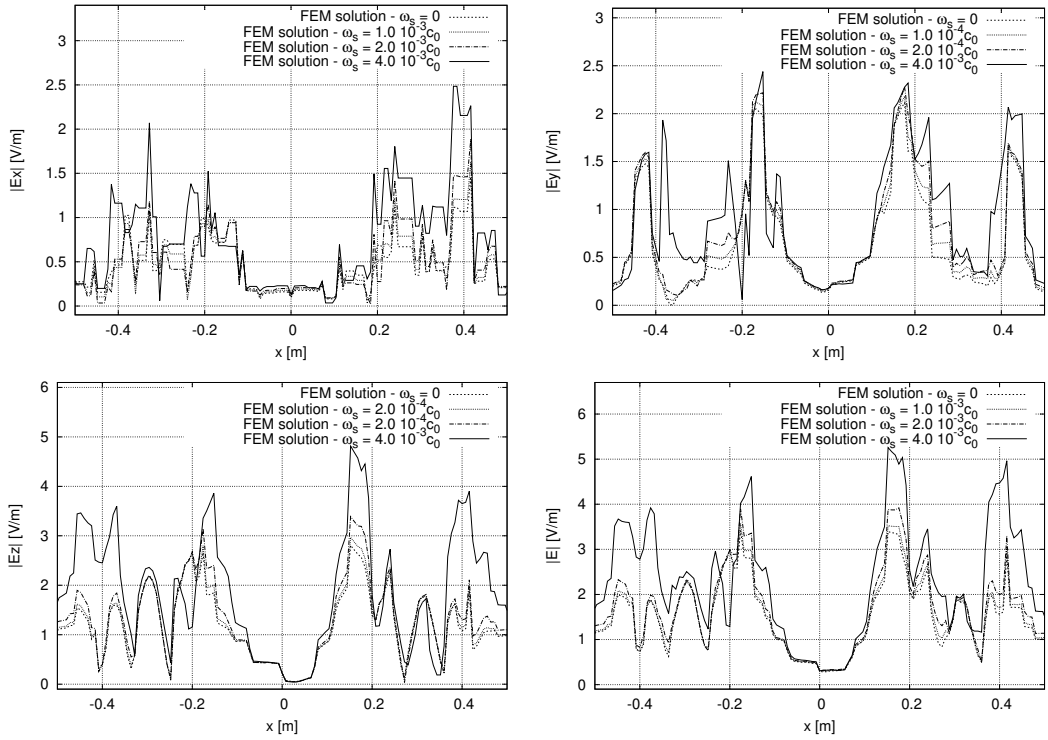

Figure 8. Magnitude of the electric field along the x-axis for different values of ω_s for rotating torus.

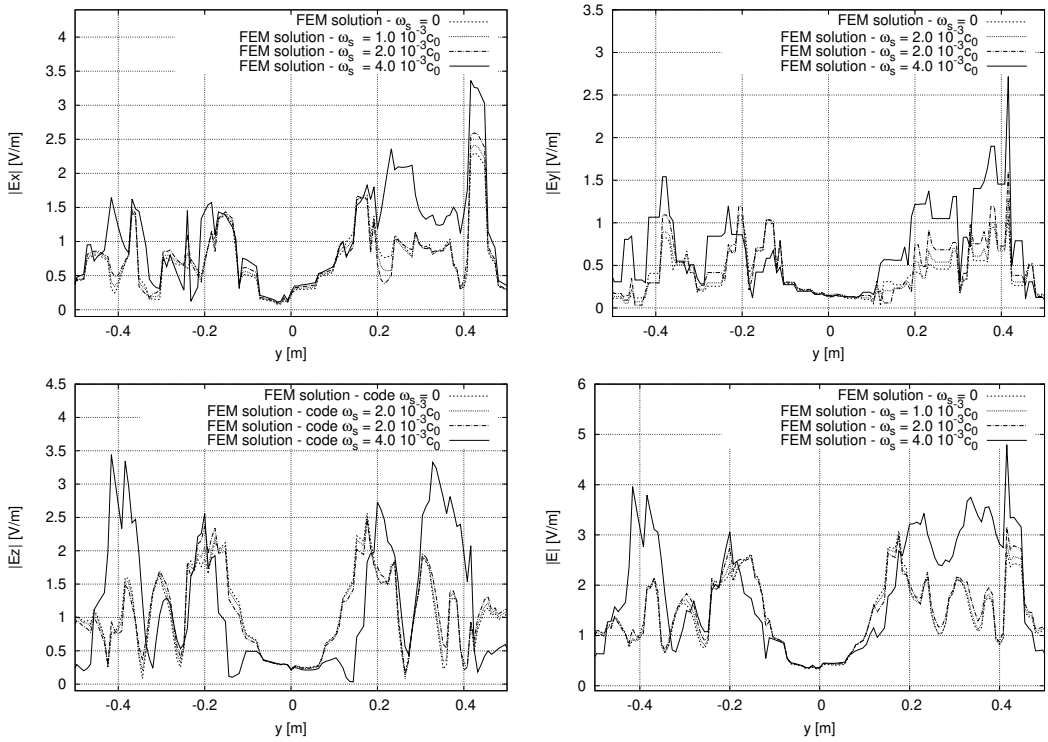

Figure 9. Magnitude of the electric field along the y-axis for different values of ω_s for rotating torus.

8. Conclusions

In this work, we have presented sufficient conditions for well posedness and finite element approximability of three-dimensional time-harmonic electromagnetic boundary value problems involving bianisotropic media. The theory is applied to electromagnetic problems involving rotating

axisymmetric objects. For some of them, the solutions are not present in the open literature and, hence, they can be used as benchmarks for other approaches.

Author Contributions: Both the authors have contributed equally to this paper. All authors have read and agreed to the published version of the manuscript.

Funding: This research received no external funding.

Conflicts of Interest: The authors declare no conflict of interest.

Appendix A

In this Appendix A, we provide Lemma A1 and the proofs of Theorem 1, Theorem 2, Theorem 4, and Lemma 1.

Lemma A1. *Any solution* $\mathbf{E}$ *of Problem 2 with* $l = 0$ *satisfies*

- $\mathbf{n} \times \mathbf{E} = 0$ *on* Γ_l *if HM3, HB2 and HB3 hold true,*
- $\mathbf{E} = 0$ *in* D *if HM3, HB2 and HM4 hold true; the same result is achieved under hypotheses HM3, HB2 and HM5 or HM3, HB2, HM6 and HM7.*

Proof. Consider $\mathbf{E}$ as the solution of Problem 2 with $l = 0$ and choose $\mathbf{v} = \mathbf{E}$ in Equation (6). Since $a(\mathbf{E}, \mathbf{E}) = 0$, we get

$$0 = Im(a(\mathbf{E}, \mathbf{E})) = -\int_\Omega (\mathbf{E}^*, \operatorname{curl} \mathbf{E}^*) A_{ss} \begin{pmatrix} \mathbf{E} \\ \operatorname{curl} \mathbf{E} \end{pmatrix} + \omega \int_\Gamma Re(Y) |\mathbf{n} \times \mathbf{E} \times \mathbf{n}|^2. \tag{A1}$$

Taking account that $\omega > 0$, if we assume HM3, HB2, and HB3, we easily get:

$$0 \geq \int_\Gamma Re(Y) |\mathbf{n} \times \mathbf{E} \times \mathbf{n}|^2 \geq \int_{\Gamma_l} Re(Y) |\mathbf{n} \times \mathbf{E} \times \mathbf{n}|^2 \geq C_{Ym} \int_{\Gamma_l} |\mathbf{n} \times \mathbf{E} \times \mathbf{n}|^2. \tag{A2}$$

Thus, under the indicated hypotheses, we can conclude that $\mathbf{n} \times \mathbf{E} = 0$ on Γ_l.
If HM3, HB2, and HM4 hold true, considering that $\omega > 0$, we get

$$0 \geq -\int_\Omega (\mathbf{E}^*, \operatorname{curl} \mathbf{E}^*) A_{ss} \begin{pmatrix} \mathbf{E} \\ \operatorname{curl} \mathbf{E} \end{pmatrix} \geq K_{dl} \int_D (|\mathbf{E}|^2 + |\operatorname{curl} \mathbf{E}|^2) \geq K_{dl} \int_D |\mathbf{E}|^2 \tag{A3}$$

and we conclude that $\mathbf{E} = 0$ in D.

The same result easily follows if we assume HM3, HB2 and HM5, since

$$0 \geq -\int_\Omega (\mathbf{E}^*, \operatorname{curl} \mathbf{E}^*) A_{ss} \begin{pmatrix} \mathbf{E} \\ \operatorname{curl} \mathbf{E} \end{pmatrix} \geq K_{el} \int_D |\mathbf{E}|^2, \tag{A4}$$

or if HM3, HB2, HM6 and HM7 hold true, since

$$0 \geq -\int_\Omega (\mathbf{E}^*, \operatorname{curl} \mathbf{E}^*) A_{ss} \begin{pmatrix} \mathbf{E} \\ \operatorname{curl} \mathbf{E} \end{pmatrix} \geq K_{ml} \int_D |\operatorname{curl} \mathbf{E}|^2 \tag{A5}$$

and taking account of $(5)_2$ with $\mathbf{J}_m = 0$, $(1)_2$ with $M = 0$, $(5)_1$ with $\mathbf{J}_e = 0$ and $(1)_1$ with $L = 0$. □

Proof of Theorem 1. By Lemma A1, there is either a subdomain D where the electric field $\mathbf{E} = 0$ or a part of the boundary, Γ_l, where $\mathbf{n} \times \mathbf{E} = 0$. We prove that the fields $\mathbf{E}$, $\mathbf{B}$, $\mathbf{H}$ and $\mathbf{D}$ are identically zero in Ω_i, for all $i \in I$, if one of the following is true:

- Ω_i is adjacent to a region Ω_k, $k \in I$, where it has already been proved that $\mathbf{E} = 0$,
- $\partial\Omega_i$ shares a non-empty, open, Lipschitz continuous part with Γ_l.

In both cases, we introduce a sufficiently small open ball $B \subset \mathbb{R}^3$ centered on a point of $\overline{\Omega}_i \cap \overline{\Omega}_k$ or on a point of $\partial\Omega_i \cap \Gamma_l$.

In both cases, we have $\mathbf{n} \times \mathbf{E} = 0$ on $B \cap \partial\Omega_i$. Then, considering the homogeneous version of (5), by $(5)_3$ we get $\mathbf{n} \times \mathbf{H} = 0$ on $B \cap \partial\Omega_i$. Then, Equations $(5)_1$ and $(5)_2$ respectively imply that the normal components $\mathbf{n} \cdot \mathbf{D} = 0$ and $\mathbf{n} \cdot \mathbf{B} = 0$ on $B \cap \partial\Omega_i$.

Now, we can extend in an analytic way, from Ω_i to $B \setminus \Omega_i$, all the components of κ, χ, γ and ν. This is possible because of HM8. In both cases, we have to consider that **E**, **B**, **H** and **D** are either trivial fields in $B \setminus \Omega_i$ (in the first of the two cases) or can be trivially extended to $B \setminus \Omega_i$ (in the second of the two cases).

Next, we can show that the fields in B are analytic in Ω_i, $\forall i \in I$. As a matter of fact:

- the fields **E**, **B**, **H**, **D** satisfy (5) in B since (5) holds true in Ω_i and in $B \setminus \overline{\Omega}_i$ for any $i \in I$,
- the fields **E**, **B**, **H**, **D** satisfy (1) in B since (1) holds true in Ω_i and in $B \setminus \overline{\Omega}_i$ for any $i \in I$,
- by using the properties of the fields on the boundary deduced above we easily conclude that in both the cases of interest $(\mathbf{E}, \mathbf{B}, \mathbf{H}, \mathbf{D}) \in H(\text{curl}, B) \times H(\text{div}^0, B) \times H(\text{curl}, B) \times H(\text{div}^0, B)$, [24] (p. 107)
- HS1 of [22] is satisfied in any case since the sources are trivial,
- for any Ω_i, $i \in I_a$, κ and ν satisfy HM1, HM5 and HM6 of [22] in B since we have verified them for $\overline{\Omega}_i$ (by HM8, HM9 and HM10 above) and all the extended quantities are at least continuous in $\overline{\Omega}_i$ (by HM8),
- for any Ω_i, $i \in I_b$, HM1, HM8 and HM9 of [22] are satisfied in B by κ, χ, γ, ν, which are extended analytically to a sufficiently small ball B, since we have verified them in $\overline{\Omega}_i$ for all $i \in I_b$ (by HM8, HM9 and HM11 above) and all the extended quantities are at least continuous in $\overline{\Omega}_i$ (by HM8),
- for any Ω_i, $i \in I_b$, HM12 implies that (7.11) of [22] is satisfied in B by κ, χ, γ, ν extended as indicated above since we have verified it in $\overline{\Omega}_i$ for all $i \in I_b$ and all the extended quantities involved are at least continuous in $\overline{\Omega}_i$ (by HM8).

Thus, by Theorems 6.4 and 7.3 of [22], we can conclude that the electromagnetic fields in B are analytic. Since they are equal to zero or can be extended to zero fields in $B \setminus \overline{\Omega}_i$, we get $\mathbf{E} = 0$, $\mathbf{B} = 0$, $\mathbf{H} = 0$, and $\mathbf{D} = 0$ in B. Once the fields are proved to be equal to zero in B, we easily see that they are zero in Ω_i by the analyticity of the indicated fields in Ω_i. This procedure can be successively applied to all subdomains allowing us to conclude that the homogeneous version of Problem 2 has only trivial solutions and hence Problem 2 admits a unique solution. □

Proof of Theorem 2. The homogeneous variational problem defined in the statement of the theorem is similar in form to the homogeneous version of the original problem. The only differences are the reversed roles of **u** and **v** and the change in sign of the imaginary part. Hence, the same proof will also work here. In particular, in the proof of Lemma A1, we can use the fact that $(a(\mathbf{E}, \mathbf{E}))^* = 0$ implies $Im\,(a(\mathbf{E}, \mathbf{E})) = 0$, which in turn implies (A1) and hence the conclusions of Lemma A1 hold also for the homogeneous variational problem defined in the statement of the theorem. The arguments for showing the unique continuation results are not affected by the sign of imaginary part of the sesquilinear form. Hence, we can conclude that $\mathbf{v} = 0$ is the only solution. □

Proof of Theorem 4. We prove Theorem 4 by contradiction, as we did in [10]. Due to the similarities with the corresponding proof presented in [10], we report here the main ideas.

As in [10], we get the result by contradiction and, thus, we assume that:

$$\exists\{\mathbf{u}_n\},\ \mathbf{u}_n \in U \text{ and } \|\mathbf{u}_n\|_U = 1\ \forall n \in \mathbb{N},\ \text{such that } \lim_{n\to\infty} \sup_{\|\mathbf{v}\|_U \leq 1} |a(\mathbf{u}_n, \mathbf{v})| = 0. \tag{A6}$$

For the space U, under hypotheses HD1–HD3, HM1–HM2, and HM13, the following Helmholtz decomposition holds true [24] (p. 86):

$$U = U_0 \oplus U_1, \tag{A7}$$

where

$$U_0 = \{\mathbf{u} \in U \,|\, \operatorname{curl} \mathbf{u} = 0 \text{ in } \Omega \text{ and } \mathbf{u} \times \mathbf{n} = 0 \text{ on } \Gamma\} \tag{A8}$$

and

$$U_1 = \{\mathbf{u} \in U \,|\, (P\mathbf{u}, \mathbf{v})_{0,\Omega} = 0 \; \forall \mathbf{v} \in U_0\}. \tag{A9}$$

Thus, for any element of the sequence satisfying (A6), we get

$$\mathbf{u}_n = \mathbf{u}_{n0} + \mathbf{u}_{n1}, \tag{A10}$$

with $\mathbf{u}_{n0} \in U_0$ and $\mathbf{u}_{n1} \in U_1$.

Under the assumed hypotheses, one easily gets:

$$\|\mathbf{u}_{n0}\|_{0,\Omega} = \|\mathbf{u}_{n0}\|_U \leq \frac{C_{PL}}{C_{PS}} \|\mathbf{u}_n\|_{0,\Omega} \leq \frac{C_{PL}}{C_{PS}} \|\mathbf{u}_n\|_U, \tag{A11}$$

$$\|\mathbf{u}_{n1}\|_U \leq \frac{C_{PS} + C_{PL}}{C_{PS}} \|\mathbf{u}_n\|_U, \tag{A12}$$

$$\lim_{n\to\infty} \|\mathbf{n} \times \mathbf{u}_n \times \mathbf{n}\|_{0,\Gamma} = 0. \tag{A13}$$

Thus, the two sequences, $\{\mathbf{u}_{n0}\}$ and $\{\mathbf{u}_{n1}\}$, subsequences of the sequence satisfying (A6), are bounded in U. Since our hypotheses guarantees that uniqueness also holds, then, on a common subsequence of indices, both $\{\mathbf{u}_{n0}\}$ and $\{\mathbf{u}_{n1}\}$ weakly converge to zero in U and, by the compact embedding of U_1 in $(L^2(\Omega))^3$, which holds true under hypothesis HM13, from $\{\mathbf{u}_{n1}\}$, we can extract a subsequence which converges strongly in $(L^2(\Omega))^3$ to $\hat{\mathbf{u}}_1$. Finally, since both weak convergence in U and strong convergence in $(L^2(\Omega))^3$ imply weak convergence in $(L^2(\Omega))^3$ to the same limit, we immediately deduce $\hat{\mathbf{u}}_1 = 0$.

By setting $\mathbf{u} = \mathbf{u}_n$ and $\mathbf{v} = \mathbf{u}_{n0}$ for any n, we get from the very definition of the sesquilinear form a:

$$C_{PS}\|\mathbf{u}_{n0}\|^2_{0,\Omega} \leq \frac{c_0}{\omega^2}|a(\mathbf{u}_n, \mathbf{u}_{n0})| + \frac{c_0 C_L}{\omega}\|\operatorname{curl} \mathbf{u}_n\|_{0,\Omega}\|\mathbf{u}_{n0}\|_{0,\Omega}. \tag{A14}$$

By the same token, by setting $\mathbf{u} = \mathbf{u}_n$ and $\mathbf{v} = \mathbf{u}_{n1}$ for any n, we deduce

$$\begin{aligned} c_0 C_{QS}\|\operatorname{curl} \mathbf{u}_{n1}\|^2_{0,\Omega} \leq \\ |a(\mathbf{u}_n, \mathbf{u}_{n1})| + \frac{\omega^2 C_{PL}}{c_0}\|\mathbf{u}_n\|_{0,\Omega}\|\mathbf{u}_{n1}\|_{0,\Omega} + \omega C_M\|\mathbf{u}_{n0}\|_{0,\Omega}\|\operatorname{curl} \mathbf{u}_{n1}\|_{0,\Omega} + \\ +\omega(C_M + C_L)\|\mathbf{u}_{n1}\|_{0,\Omega}\|\operatorname{curl} \mathbf{u}_{n1}\|_{0,\Omega} + \omega C_{YL}\|\mathbf{n} \times \mathbf{u}_{n1} \times \mathbf{n}\|^2_{0,\Gamma}. \end{aligned} \tag{A15}$$

Now, taking into account that $\{\mathbf{u}_{n0}\}$ and $\{\mathbf{u}_{n1}\}$ are bounded in U, $\|\mathbf{u}_{n1}\|_{0,\Omega} \to 0$ on a subsequence, $\|(\mathbf{n} \times \mathbf{u}_{n1} \times \mathbf{n})\|_{0,\Gamma} \to 0$, by using inequalities (A14) and (A15), we deduce that we cannot find a subsequence such that either $\{\mathbf{u}_{n0}\}$ or $\{\operatorname{curl} \mathbf{u}_{n1}\}$ converges to zero in $(L^2(\Omega))^3$. As a matter of fact, if one of them did converge to zero in $(L^2(\Omega))^3$, then both should do and we would obtain that $\{\mathbf{u}_n\}$ should converge to zero in U against the hypothesis.

Then, we can find a subsequence giving $\|\mathbf{u}_{n1}\|_{0,\Omega} \to 0$ and $\|\mathbf{u}_{n0}\|_{0,\Omega} \geq \epsilon > 0$. On this subsequence, from inequality (A14), we get

$$\|\mathbf{u}_{n0}\|_{0,\Omega} \leq \frac{c_0}{\omega^2 C_{PS}}|a(\mathbf{u}_n, \frac{\mathbf{u}_{n0}}{\|\mathbf{u}_{n0}\|_{0,\Omega}})| + \frac{c_0 C_L}{\omega C_{PS}}\|\operatorname{curl} \mathbf{u}_{n1}\|_{0,\Omega}. \tag{A16}$$

By substituting the right-hand side of (A16) for $\|\mathbf{u}_{n0}\|_{0,\Omega}$ in inequality (A15), we deduce

$$\begin{aligned} & c_0\left(C_{QS}-\frac{C_L C_M}{C_{PS}}\right)\|\mathrm{curl}\,\mathbf{u}_{n1}\|_{0,\Omega}^2 \leq \\ & \frac{C_{PS}+C_{PL}}{C_{PS}}\left|a\left(\mathbf{u}_n,\frac{C_{PS}}{C_{PS}+C_{PL}}\mathbf{u}_{n1}\right)\right|+\frac{\omega^2 C_{PL}}{c_0}\|\mathbf{u}_n\|_{0,\Omega}\|\mathbf{u}_{n1}\|_{0,\Omega}+ \\ & +\omega(C_M+C_L)\|\mathbf{u}_{n1}\|_{0,\Omega}\|\mathrm{curl}\,\mathbf{u}_{n1}\|_{0,\Omega}+\omega C_{YL}\|(\mathbf{n}\times\mathbf{u}_{n1}\times\mathbf{n})\|_{0,\Gamma}^2+ \\ & +\frac{c_0 C_M}{\omega C_{PS}}\left|a\left(\mathbf{u}_n,\frac{\mathbf{u}_{n0}}{\|\mathbf{u}_{n0}\|_{0,\Omega}}\right)\right|\|\mathrm{curl}\,\mathbf{u}_{n1}\|_{0,\Omega}. \end{aligned} \tag{A17}$$

The right-hand side of inequality (A17) converges to zero on the indicated subsequence and, by hypothesis HM15, we get $\|\mathrm{curl}\,\mathbf{u}_{n1}\|_{0,\Omega}\to 0$, which is against the starting hypothesis. □

Proof of Lemma 1. We have to analyse just the case when Ω_{el} is neither the whole Ω nor the empty set. For all $\mathbf{u}\in(L^2(\Omega))^3$, we have

$$\begin{aligned} |(P\mathbf{u},\mathbf{u})_{0,\Omega}|^2 &= \left|\int_\Omega \mathbf{u}^* P_s\mathbf{u}-j\int_\Omega \mathbf{u}^* P_{ss}\mathbf{u}\right|^2 = \\ &= \left(\int_\Omega \mathbf{u}^* P_s\mathbf{u}\right)^2+\left(\int_\Omega \mathbf{u}^* P_{ss}\mathbf{u}\right)^2 = \\ &= \left(\int_{\Omega\setminus\Omega_{el}} \mathbf{u}^* P_s\mathbf{u}-\int_{\Omega_{el}} -\mathbf{u}^* P_s\mathbf{u}\right)^2+\left(\int_{\Omega_{el}} \mathbf{u}^* P_{ss}\mathbf{u}+\int_{\Omega\setminus\Omega_{el}} \mathbf{u}^* P_{ss}\mathbf{u}\right)^2. \end{aligned} \tag{A18}$$

Under assumption HM3, by using Lemma B.1 of [9] with $K_1=K_2=0$, we get that P_{ss} is positive semi definite in Ω_i, $\forall i\in I$. Moreover, since Ω_{el} is the union of the subdomains Ω_i of Ω where P_{ss} is uniformly positive definite, we get

$$|(P\mathbf{u},\mathbf{u})_{0,\Omega}|^2 \geq \left(\int_{\Omega\setminus\Omega_{el}} \mathbf{u}^* P_s\mathbf{u}-\int_{\Omega_{el}} -\mathbf{u}^* P_s\mathbf{u}\right)^2+C_1^2||\mathbf{u}||_{0,\Omega_{el}}^4. \tag{A19}$$

However, for all $a,b\in\mathbb{R}$, for any $\alpha>0$, we have

$$(a-b)^2\geq(1-\alpha)a^2+(1-\frac{1}{\alpha})b^2. \tag{A20}$$

Then, using the above inequality for the first addend of the right-hand side of Equation (A19), we get

$$|(P\mathbf{u},\mathbf{u})_{0,\Omega}|^2 \geq (1-\alpha)\left(\int_{\Omega\setminus\Omega_{el}} \mathbf{u}^* P_s\mathbf{u}\right)^2+(1-\frac{1}{\alpha})\left(\int_{\Omega_{el}} \mathbf{u}^* P_s\mathbf{u}\right)^2+C_1^2||\mathbf{u}||_{0,\Omega_{el}}^4. \tag{A21}$$

The validity of assumption HM2 guarantees that inequality (28) holds true. Then, by taking account that $1-\frac{1}{\alpha}<0$ for all $\alpha\in(0,1)$, we get

$$|(P\mathbf{u},\mathbf{u})_{0,\Omega}| \geq (1-\alpha)\left(\int_{\Omega\setminus\Omega_{el}} \mathbf{u}^* P_s\mathbf{u}\right)^2+(C_1^2+(1-\frac{1}{\alpha})C_3^2)||\mathbf{u}||_{0,\Omega_{el}}^4. \tag{A22}$$

By using (25), we then deduce

$$|(P\mathbf{u},\mathbf{u})_{0,\Omega}|^2 \geq (1-\alpha)C_5^2||\mathbf{u}||_{0,\Omega\setminus\Omega_{el}}^4+(C_1^2+(1-\frac{1}{\alpha})C_3^2)||\mathbf{u}||_{0,\Omega_{el}}^4. \tag{A23}$$

By defining $1 > \alpha > \frac{C_3^2}{C_1^2+C_3^2} > 0$, we have that both terms in (A23) are positive. As a matter of fact, we can think of the right-hand side of (A23) as $s^2 + t^2$, $s, t \in \mathbb{R}$, and, since $s^2 + t^2 \geq \frac{(s+t)^2}{2}$, we get

$$
\begin{aligned}
|(P\mathbf{u}, \mathbf{u})_{0,\Omega}|^2 \geq \frac{1}{2}\left(\sqrt{(1-\alpha)}\, C_5 ||\mathbf{u}||^2_{0,\Omega\setminus\Omega_{el}} + \sqrt{C_1^2 + (1-\frac{1}{\alpha})C_3^2}\, ||\mathbf{u}||^2_{0,\Omega_{el}}\right)^2 \geq \\
\geq \frac{1}{2}\left(\min\left(\sqrt{(1-\alpha)}\, C_5, \sqrt{C_1^2 + (1-\frac{1}{\alpha})C_3^2}\right)\right)^2 \left(||\mathbf{u}||^2_{0,\Omega\setminus\Omega_{el}} + ||\mathbf{u}||^2_{0,\Omega_{el}}\right)^2 = \\
= \frac{1}{2}\min\left((1-\alpha)C_5^2, C_1^2 + (1-\frac{1}{\alpha})C_3^2\right) ||\mathbf{u}||^4_{0,\Omega}.
\end{aligned}
\tag{A24}
$$

□

References

1. De Zutter, D. Scattering by a rotating dielectric sphere. *IEEE Trans. Antennas Propag.* **1980**, *28*, 643–651. [CrossRef]
2. Van Bladel, J. Rotating dielectric sphere in a low-frequency field. *Proc. IEEE* **1979**, *67*, 1654–1655. [CrossRef]
3. Cheng, D.K.; Kong, J.A. Covariant descriptions of bianisotropic media. *Proc. IEEE* **1968**, *56*, 248–251. [CrossRef]
4. Sommerfeld, A. *Electrodynamics*; Lectures on Theoretical Physics; Academic Press: New York, NY, USA, 1952.
5. Kraft, M.; Braun, A.; Luo, Y.; Maier, S.A.; Pendry, J.B. Bianisotropy and magnetism in plasmonic gratings. *ACS Photonics* **2016**, *3*, 764–769. [CrossRef]
6. Yazdi, M.; Albooyeh, M.; Alaee, R.; Asadchy, V.; Komjani, N.; Rockstuhl, C.; Simovski, C.R.; Tretyakov, S. A bianisotropic metasurface with resonant asymmetric absorption. *IEEE Trans. Antennas Propag.* **2015**, *63*, 3004–3015. [CrossRef]
7. Kildishev, A.V.; Borneman, J.D.; Ni, X.; Shalaev, V.M.; Drachev, V.P. Bianisotropic effective parameters of optical metamagnetics and negative-index materials. *Proc. IEEE* **2011**, *99*, 1691–1700. [CrossRef]
8. Kriegler, C.E.; Rill, M.S.; Linden, S.; Wegener, M. Bianisotropic photonic metamaterials. *IEEE J. Sel. Top. Quantum Electron.* **2010**, *16*, 367–375. [CrossRef]
9. Fernandes, P.; Raffetto, M. Well-posedness and finite element approximability of time-harmonic electromagnetic boundary value problems involving bianisotropic materials and metamaterials. *Math. Model. Methods Appl. Sci.* **2009**, *19*, 2299–2335. [CrossRef]
10. Brignone, M.; Raffetto, M. Well posedness and finite element approximability of two-dimensional time-harmonic electromagnetic problems involving non-conducting moving objects with stationary boundaries. *ESAIM Math. Model. Numer. Anal.* **2015**, *49*, 1157–1192. [CrossRef]
11. Ioannidis, A.D.; Kristensson, G.; Stratis, I.G. On the well-posedness of the Maxwell system for linear bianisotropic media. *SIAM J. Math. Anal.* **2012**, *44*, 2459–2473. [CrossRef]
12. Cocquet, P.; Mazet, P.; Mouysset, V. On the existence and uniqueness of a solution for some frequency-dependent partial differential equations coming from the modeling of metamaterials. *SIAM J. Math. Anal.* **2012**, *44*, 3806–3833. [CrossRef]
13. Costen, R.C.; Adamson, D. Three-dimensional derivation of the electrodynamic jump conditions and momentum-energy laws at a moving boundary. *Proc. IEEE* **1965**, *53*, 1181–1196. [CrossRef]
14. Bilotti, F.; Vegni, L.; Toscano, A. Radiation and scattering features of patch antennas with bianisotropic substrates. *IEEE Trans. Antennas Propag.* **2003**, *51*, 449–456. [CrossRef]
15. Cheng, X.; Chen, H.; Wu, B.I.; Kong, J.A. Cloak for Bianisotropic and Moving Media. *Prog. Electromagn. Res.* **2009**, *89*, 199–212. [CrossRef]
16. Alotto, P.; Codecasa, L. A fit formulation of bianisotropic materials over polyhedral grids. *IEEE Trans. Magn.* **2014**, *50*, 349–352. [CrossRef]
17. Wu, T.X.; Jaggard, D.L. A comprehensive study of discontinuities in chirowaveguides. *IEEE Trans. Microw. Theory Tech.* **2002**, *50*, 2320–2330. [CrossRef]

18. Kalarickel Ramakrishnan, P.; Raffetto, M. Accuracy of finite element approximations for two-dimensional time-harmonic electromagnetic boundary value problems involving non-conducting moving objects with stationary boundaries. *ACES J.* **2018**, *33*, 585–596.
19. Van Bladel, J.G. *Electromagnetic Fields*, 2nd ed.; IEEE Press: Piscataway, NJ, USA, 2007.
20. Harrington, R.F. *Time-Harmonic Electromagnetic Fields*; McGraw-Hill: New York, NY, USA, 1961.
21. Kong, J.A. *Theory of Electromagnetic Waves*; Wiley: New York, NY, USA, 1975.
22. Fernandes, P.; Ottonello, M.; Raffetto, M. Regularity of time-harmonic electromagnetic fields in the interior of bianisotropic materials and metamaterials. *IMA J. Appl. Math.* **2014**, *79*, 54–93. [CrossRef]
23. Girault, V.; Raviart, P.A. *Finite Element Methods for Navier–Stokes Equations*; Springer–Verlag: Berlin, Germany, 1986.
24. Monk, P. *Finite Element Methods for Maxwell's Equations*; Oxford Science Publications: Oxford, UK, 2003.
25. Taylor, A.E. *Introduction to Functional Analysis*; John Wiley & Sons: New York, NY, USA, 1958.
26. Leis, R., *Trends in Applications of Pure Mathematics to Mechanics*; Chapter Exterior Boundary-Value Problems In Mathematical Physics; Pitman: London, UK, 1979; Volume 11, pp. 187–203.
27. Hazard, C.; Lenoir, M. On the solution of time-harmonic scattering problems for Maxwell's equations. *SIAM J. Math. Anal.* **1996**, *27*, 1597–1630. [CrossRef]
28. Alonso, A.; Raffetto, M. Unique solvability for electromagnetic boundary value problems in the presence of partly lossy inhomogeneous anisotropic media and mixed boundary conditions. *Math. Model. Methods Appl. Sci.* **2003**, *13*, 597–611. [CrossRef]
29. Ciarlet, P.G. *The Finite Element Method for Elliptic Problems*; North-Holland: Amsterdam, The Netherlands, 1978.
30. Caorsi, S.; Fernandes, P.; Raffetto, M. On the convergence of Galerkin finite element approximations of electromagnetic eigenproblems. *SIAM J. Numer. Anal.* **2000**, *38*, 580–607. [CrossRef]
31. Caorsi, S.; Fernandes, P.; Raffetto, M. Spurious-free approximations of electromagnetic eigenproblems by means of Nedelec-type elements. *Math. Model. Numer. Anal.* **2001**, *35*, 331–354. [CrossRef]
32. Jin, J. *The Finite Element Method in Electromagnetics*; John Wiley & Sons: New York, NY, USA, 1993.
33. Barrett, R.; Berry, M.; Chan, T.F.; Demmel, J.; Donato, J.; Dongarra, J.; Eijkhout, V.; Pozo, R.; Romine, C.; der Vorst, H.V. *Templates for the Solution of Linear Systems: Building Blocks for Iterative Methods*, 2nd ed.; SIAM: Philadelphia, PA, USA, 1994.
34. Fernandes, P.; Raffetto, M. Existence, uniqueness and finite element approximation of the solution of time-harmonic electromagnetic boundary value problems involving metamaterials. *COMPEL* **2005**, *24*, 1450–1469. [CrossRef]
35. De Zutter, D. Scattering by a rotating circular cylinder with finite conductivity. *IEEE Trans. Antennas Propag.* **1983**, *31*, 166–169. [CrossRef]
36. Brignone, M.; Ramakrishnan, P.K.; Raffetto, M. A first numerical assessment of the reliability of finite element simulators for time-harmonic electromagnetic problems involving rotating axisymmetric objects. In Proceedings of the 2016 URSI International Symposium on Electromagnetic Theory (EMTS), Espoo, Finland, 14 August 2016; pp. 787–790.
37. Pastorino, M.; Raffetto, M.; Randazzo, A. Electromagnetic inverse scattering of axially moving cylindrical targets. *IEEE Trans. Geosci. Remote Sens.* **2015**, *53*, 1452–1462. [CrossRef]
38. Brignone, M.; Gragnani, G.L.; Pastorino, M.; Raffetto, M.; Randazzo, A. Noise limitations on the recovery of average values of velocity profiles in pipelines by simple imaging systems. *IEEE Geosci. Remote Sens. Lett.* **2016**, *13*, 1340–1344. [CrossRef]